

THE

Journal

OF THE AMERICAN
LEATHER CHEMISTS ASSOCIATION

October 2021

Vol. CXVI, No.10

JALCA 116(10), 337-376, 2021



116th Annual Convention

to be held at the
Eaglewood Resort & Spa
1401 Nordic Road
Itasca, IL 60143

DATE CHANGE:
June 21-24, 2022

For more information go to:
[leatherchemists.org/
annual_convention.asp](http://leatherchemists.org/annual_convention.asp)

Contents

- Solid State NMR Analysis for Hide Powder Tanned by Aluminum, Silicon and Phosphorus Tanning Agents before and after Hydrothermal Denaturation**
by Jun Liu, Da-hai He, Hua-lin Chen and Ke-yi Ding 339
- Fabrication of Composite Films Based on Chitosan and Vegetable-Tanned Collagen Fibers Crosslinked with Genipin**
by Jie Liu, Yanchun Liu, Eleanor M. Brown, Zhengxin Ma,
and Cheng-Kung Liu 345
- Avoiding the Production of Polluting and Toxic Chemicals in the Tanning Process**
by Josep M. Morera, Esther Bartolí, Patricia Rojas and Luisa F. Cabeza 359
- Role of Anionic Chromium Species in Leather Tanning**
by Abhinandan Kumar, Jaya Prakash Alla, Deepika Arathanaikotti,
Ashok Raj J. and Chandrababu N. K. 368
- Lifelines** 375
- Obituary: David Rabinovich**..... 376

Distributed by



An imprint of the University of Cincinnati Press

ISSN: 0002-9726

Communications for Journal Publication

Manuscripts, Technical Notes and Trade News Releases should contact:
MR. STEVEN D. LANGE, Journal Editor, 1314 50th Street, Suite 103, Lubbock, TX 79412, USA
E-mail: jalcaeditor@gmail.com Mobile phone: (814) 414-5689

Contributors should consult the Journal Publication Policy at:
http://www.leatherchemists.org/journal_publication_policy.asp

Beamhouse efficiency takes perfect balance.

Making leather on time, on spec and within budget requires a careful balance of chemistry and process. Buckman enables tanneries to master that balance with our comprehensive Beamhouse & Tanyard Systems. They include advanced chemistries that not only protect the hide but also maximize the effectiveness of each process, level out the differences in raw materials and reduce variations in batch processing. The result is cleaner, flatter pelts. More uniform characteristics. And improved area yield.

In addition, we offer unsurpassed expertise and technical support to help solve processing problems and reduce environmental impact with chemistries that penetrate faster, save processing time, improve effluent and enhance safety.

With Buckman Beamhouse & Tanyard Systems, tanneries can get more consistent quality and more consistent savings. Maintain the perfect balance. Connect with a Buckman representative or visit us at Buckman.com.

1945
2020 **Buckman75**

JOURNAL OF THE AMERICAN LEATHER CHEMISTS ASSOCIATION

*Proceedings, Reports, Notices, and News
of the*
AMERICAN LEATHER CHEMISTS ASSOCIATION

OFFICERS

MIKE BLEY, *President*
Eagle Ottawa – Lear
2930 Auburn Road
Rochester Hills, MI 48309

JOSEPH HOEFLER, *Vice-President*
The Dow Chemical Company
400 Arcola Rd.
Collegeville, PA 19426

COUNCILORS

Shawn Brown
Quaker Color
201 S. Hellertown Ave.
Quakertown, PA 18951

Steve Lange
Leather Research Laboratory
University of Cincinnati
5997 Center Hill Ave., Bldg. C
Cincinnati, OH 45224

John Rodden
Union Specialties, Inc.
3 Malcolm Hoyt Dr.
Newburyport, MA 01950

Jose Luis Gallegos
Elementis LTP
546 S. Water St.
Milwaukee, WI 53204

LeRoy Lehman
LANXESS Corporation
9501 Tallwood Dr.
Indian Trail, NC 28079

Marcelo Fraga de Sousa
Buckman North America
1256 N. McLean Blvd.
Memphis, TN 38108

EDITORIAL BOARD

Dr. Meral Birbir
Biology Department
Faculty of Arts and Sciences
Marmara University
Istanbul, Turkey

Chris Black
Consultant
St. Joseph, Missouri

Dr. Eleanor M. Brown
Eastern Regional
Research Center
U.S. Department of Agriculture
Wyndmoor, Pennsylvania

Dr. Anton Ela'mma
Retired
Perkiomenville, Pennsylvania

Cietta Fambrough
Leather Research Laboratory
University of Cincinnati
Cincinnati, Ohio

Mainul Haque
ALCA Education
Committee Chairman
Rochester Hills, Michigan

Joseph Hoefler
Dow Chemical Company
Collegeville, Pennsylvania

Elton Hurlow
Buckman International
Memphis, Tennessee

Prasad V. Inaganti
Wickett and Craig of America
Curwensville, Pennsylvania

Dr. Tariq M. Khan
Research Fellow, Machine Learning
Faculty of Sci Eng & Built Env
School of Info Technology
Geelong Waurin Ponds Campus
Victoria, Australia

Nick Latona
Eastern Regional Research Center
U.S. Department of Agriculture
Wyndmoor, Pennsylvania

Dr. Xue-pin Liao
National Engineering Centre for Clean
Technology of Leather Manufacture
Sichuan University
Chengdu, China

Dr. Cheng-Kung Liu
Eastern Regional Research Center
U.S. Department of Agriculture
Wyndmoor, Pennsylvania

Dr. Rafea Naffa
New Zealand Leather & Shoe
Research Association Inc. (LASRA*)
Palmerston North, New Zealand

Edwin Nungesser
Dow Chemical Company
Collegeville, Pennsylvania

Dr. Benson Ongarora
Department of Chemistry
Dedan Kimathi University of Technology
Nyeri, Kenya

Lucas Paddock
Chemtan Company, Inc.
Exeter, New Hampshire

Dr. J. Raghava Rao
Central Leather
Research Institute
Chennai, India

Andreas W. Rhein
Tyson Foods, Inc.
Dakota Dunes, South Dakota

Dr. Majher Sarker
Eastern Regional
Research Center
U.S. Department of Agriculture
Wyndmoor, Pennsylvania

Dr. Bi Shi
National Engineering Laboratory
Sichuan University
Chengdu, China

Dr. Palanisamy Thanikaivelan
Central Leather
Research Institute
Chennai, India

Dr. Xiang Zhang
Genomics, Epigenomics and
Sequencing Core
University of Cincinnati
Cincinnati, Ohio

Dr. Luis A. Zugno
Buckman International
Memphis, Tennessee

PAST PRESIDENTS

G. A. KERR, W. H. TEAS, H. C. REED, J. H. YOCUM, F. H. SMALL, H. T. WILSON, J. H. RUSSELL, F. P. VEITCH, W. K. ALSOP, L. E. LEVI, C. R. OBERFELL, R. W. GRIFFITH, C. C. SMOOT, III, J. S. ROGERS, LLOYD BALDERSON, J. A. WILSON, R. W. FREY, G. D. MCLAUGHLIN, FRED O'FLAHERTY, A. C. ORTHMANN, H. B. MERRILL, V. J. MLEJNEK, J. H. HIGHBERGER, DEAN WILLIAMS, T. F. OBERLANDER, A. H. WINHEIM, R. M. KOPPENHOEFER, H. G. TURLEY, E. S. FLINN, E. B. THORSTENSEN, M. MAESER, R. G. HENRICH, R. STUBBINGS, D. MEO, JR., R. M. LOLLAR, B. A. GROTA, M. H. BATTLES, J. NAGHSKI, T. C. THORSTENSEN, J. J. TANCOS, W. E. DOOLEY, J. M. CONSTANTIN, L. K. BARBER, J. J. TANCOS, W. C. PRENTISS, S. H. FAIRHELLER, M. SIEGLER, F. H. RUTLAND, D.G. BAILEY, R. A. LAUNDER, B. D. MILLER, G. W. HANSON, D. G. MORRISON, R. F. WHITE, E. L. HURLOW, M. M. TAYLOR, J. F. LEVY, D. T. DIDATO, R. HAMMOND, D. G. MORRISON, W. N. MULLINIX, D. C. SHELLY, W. N. MARMER, S. S. YANEK, D. LEBLANC, C.G. KEYSER, A.W. RHEIN, S. GILBERG, S. LANGE, S. DRAYNA, D. PETERS

THE JOURNAL OF THE AMERICAN LEATHER CHEMISTS ASSOCIATION (USPS #019-334) is published monthly by The American Leather Chemists Association, 1314 50th Street, Suite 103, Lubbock, Texas 79412. Telephone (806)744-1798 Fax (806)744-1785. Single copy price: \$8.50 members, \$17.00 non-member. Subscriptions: \$185 for hard copy plus postage and handling of \$60 for domestic subscribers and \$70 for foreign subscribers; \$185 for ezine only; and \$205 for hard copy and ezine plus postage and handling of \$60 for domestic subscribers and \$70 for foreign subscribers.

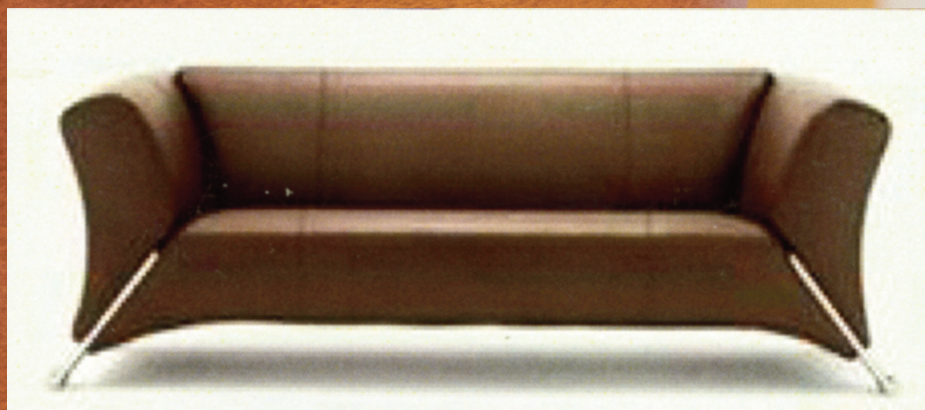
Periodical Postage paid at Lubbock, Texas and additional mailing offices. Postmaster send change of addresses to The American Leather Chemists Association, 1314 50th Street, Suite 103, Lubbock, Texas 79412.

LEATHER

AVELLISYNCO



Selected Dyestuffs



 **CHEMTAN**

17 Noble Farm Drive • Lee, NH 03861 (Office)
57 Hampton Road • Exeter, NH 03833 (Manufacturing)
Tel: (603) 772-3741 • Fax: (603) 772-0796
www.CHEMTAN.com

Solid State NMR Analysis for Hide Powder Tanned by Aluminum, Silicon and Phosphorus Tanning Agents before and after Hydrothermal Denaturation

by

Jun Liu,¹ Da-hai He,² Hua-lin Chen¹ and Ke-yi Ding^{1,3*}

¹College of Chemistry & Environment, Southwest Minzu University, Chengdu, 610041, China;

²College of Pharmacy, Southwest Minzu University, Chengdu, 610041, China;

³College of Life Science, Dalian Minzu University, Dalian, 116600, China)

Abstract

In order to investigate the change of chemical bonds between tanning agents and collagen molecules directly, hide powder tanned by aluminum, silicon and phosphorus tanning agents were prepared. The chemical shifts of Al, Si and P in tanned hide powder were analyzed by solid-state ²⁷Al NMR, ²⁹Si NMR and ³¹P NMR. The results showed that, the chemical shift of Al in aluminum tanned hide powder which interacted with collagen molecules through coordination bond could be regarded as unchanging after hydrothermal denaturation (only slightly moved to high field area). The chemical shift of Si in silicon tanned hide powder which interacted with collagen molecules through hydrogen bond did not change after hydrothermal denaturation. The chemical shift of P in phosphorus tanned hide powder, which interacted with collagen molecules through covalent bond, was obviously shifted to the high field area after hydrothermal denaturation.

Introduction

Tanning is the essential process to transform hides into leather. If tanning is regarded as a kind of chemical reaction, its reactants are raw hides (mainly composed of type I collagen) and various tanning agents (metal tanning agents such as chromium salt and aluminum salt; vegetable tanning agents such as various tannin extracts; organic tanning agents such as glutaraldehyde and oxazolidine; etc.). It is consensus that leather should possess four characteristics after tanning process: (1) an improved hydrothermal stability; (2) resistance of microbial erosion; (3) its hand feeling, color and smell are different from raw hide; (4) it will not be turned back to raw hide after repeated drying and wetting cycles. Because the hydrothermal shrinkage temperature (T_s) of leather is the key index to characterize the tanning effect, and it has a positive correlation with the other three properties,¹ therefore, the study on tanning mechanism and tanning theory usually focuses on the research of the hydrothermal stability of leather.

The key to study tanning mechanism of a certain tanning agent is to find out how the tanning agent improves the hydrothermal stability

of collagen. This requires a clear understanding of the molecular structure of collagen and the composition and structure of the tanning agent. Only after that, the chemical reaction mechanism between them could be studied. Due to the complex and insoluble structure of collagen macromolecules, as well as the complexity and diversity of the composition and structure of various tanning agents, it is very difficult to study the tanning mechanism. As noted by Brown et al, "tanning is more suitably described than defined; tanning chemistry is more like art than science".² So far, according to the research on tanning mechanism of various tanning agents, a lot of theories, such as adsorption, coating, salt bond (ionic bond), hydrophobic bond, hydrogen bond, covalent bond and coordination bond theory, have been put forward.³

In addition to studying the chemical reaction between tanning agents and collagen molecules, another method for the research of tanning mechanism, i.e., the combination mode of tanning agent and collagen, which can be inferred via characterizing the tanned collagen by spectral analysis, could be adopted. At present, the main characterization methods are infrared spectroscopy,⁴ crystal diffraction,⁵ Raman spectroscopy,⁶ molecular simulation,⁷ nuclear magnetic resonance (NMR),^{8,9} etc. Infrared spectroscopy and Raman spectroscopy mainly reflect the hydrogen bond between collagen, which is not enough to fully investigate the interaction between tanning agents and collagen. Crystal diffraction experiment is to measure the distance between collagen molecules by measuring the diffraction angle, which could only reflect the presence of hydrogen bond between collagen molecules. Although molecular simulation can reflect the interaction between collagen and tanning agent, it is not a real material and is still different from the actual situation. Adopting ³¹P NMR, Li Ya et al.⁸ studied the reaction of tetrahydroxymethyl phosphorus chloride (THPC) with polycaprolactam, polyvinyl alcohol and ethylenediamine to simulate the reaction of amide group, hydroxyl group and amino group of collagen with THPC, but it is still not the real reaction of collagen with THPC.

If the molecular structure of tanning agents can be characterized by NMR, the tanning mechanism can be directly inferred by analyzing

*Corresponding author email: dingkeyi@dlnu.edu.cn

Manuscript received March 29, 2021, accepted for publication April 25, 2021.

the change of chemical shift of the characterized element in the tanning agent before and after the hydrothermal denaturation of tanned collagen. Covington et al.¹⁰ studied the chemical shift of aluminum (III) before and after hydrothermal denaturation of collagen tanned with aluminum salt by solid-state ²⁷Al NMR, and their results showed that the chemical shift of Al³⁺ did not change. They inferred that there is no cross-linking between aluminum complex and collagen molecules through coordination bonds, and they took this fact as a counter evidence to the cross-linking theory.

In this paper, tanned collagen samples were prepared by aluminum tanning agent, silicon tanning agent and phosphorus tanning agent. The chemical shifts of aluminum, silicon and phosphorus in tanned samples before and after hydrothermal denaturation were analyzed by solid-state NMR. The purpose of this work is to clarify the changes of the interaction between tanning agent and collagen molecules during the process of hydrothermal shrinkage, and to provide experimental basis for the study of tanning theory.

Experimental

Materials and Instruments

Sodium chloride, aluminum sulfate octadecahydrate, citric acid dihydrate, sodium bicarbonate, sulfuric acid, sodium silicate, γ -(2,3-epoxypropoxy) propyl trimethoxysilane (GPTMS), tetrahydroxymethyl phosphorus chloride (THPC), formic acid and other reagents are analytically pure, purchased from Chengdu Kelong Chemical Co., Ltd. White hide powder is provided by Leather Department of Sichuan University. DSC analysis was performed on a differential thermal scanner (Q2000, TA company, USA) and solid-state NMR analysis was performed on 11.7T Bruker Avance III-400.

Aluminum Tanning

Preparation of Tanning Solution¹¹

Take 9.6632 g aluminum sulfate octadecahydrate, fix the volume in 100 mL volumetric flask (No. 1), and draw 33.3 mL from it into another 100 mL volumetric flask (No. 2). Weigh 2.6950g sodium citrate and put the same constant volume into a 100 mL volumetric flask. Take out 54.5 mL and add it into No. 2 conical flask. Add NaOH solution (0.5 mol/L) to adjust pH to 3.5 and place it for more than 24 h.

Tanning Process¹¹

Weigh 0.5 g hide powder into a 25 mL conical flask, add 8 mL NaCl solution (1 mol/L), adjust pH to 2.5 with 1 mol/L formic acid solution, and oscillate at 30°C for 36 h. Then, take 10 mL aluminum tanning solution from No.2 volumetric flask, add it into the conical flask, and vibrate at 30°C for about 30 h. After that, NaHCO₃ solution (10%, w/w) was added in several times, pH was adjusted to 5 within 2 hours, and then oscillated at 30°C for 10 hours. Filter out the hide powder with gauze and keep it in a sealed bag for testing.

Phosphorous Tanning¹²

Put 0.5 g hide powder into a 25 mL conical flask, add 8 mL NaCl solution (1mol/L), and shake overnight at 25°C. Then, add 60% THPC solution in the conical flask, and shake at 40°C for 1 h. After that, add NaHCO₃ solution (10%, w/w) to adjust the pH to 10.0, and continue to oscillate for 1.5 h at 40°C. After standing for 12 h, wash with water, filter out the hide powder with gauze, and store in sealed bag for testing.

Silicon Tanning

Preparation of Silicic Acid Tanning Solution¹³

Sulfuric acid and sodium silicate were used as raw materials to prepare silicic acid solution. Specifically, first, dilute concentrated sulfuric acid to dilute sulfuric acid according to the mass ratio of 1:1, and then cool to room temperature for standby. The sodium silicate weighed according to the mass concentration of 10% is dissolved in water to form a clear and transparent solution. Then, under the condition of stirring, slowly add sodium silicate solution into dilute sulfuric acid solution according to the stoichiometric ratio of sodium silicate to sulfuric acid as 1:1.1, stir evenly, stand still and cool to room temperature before use. The mass concentration of the achieved silica tanning solution is about 3% (equivalent to SiO₂), pH is 2.0-2.5.

Tanning Process¹³

Weigh 0.5 g hide powder into a 25 mL conical flask, add 8ml NaCl solution (1mol/L), adjust pH to about 2.0 with 1 mol/L formic acid solution, and oscillate at 30°C for about 36 h. Then, add 15% γ - (2.3-epoxy propoxy) propyl trimethoxysilane (GPTMS) by the weight of hide powder, shake for 1 h, and then add 15% silica tanning solution (equivalent to SiO₂) by the weight of hide powder, shake for 5 h. After that, NaHCO₃ solution (10%,w/w) was added in several times, pH was adjusted to 5 within 2 h, and then oscillated at 30°C for 10 h. Filter out the hide powder with gauze and keep it in a sealed bag for testing.

DSC Analysis

DSC analysis was performed on Q2000, TA company, USA. Take 5 mg of white hide powder (reference sample) and samples tanned with aluminum, silicon, phosphorus tanning agents respectively, seal them in aluminum plate. The scanning temperature was 25~120°C, the heating rate was 5°C /min, the flow rate of nitrogen was 10mL / min, and the onset temperature of DSC curve was taken as the hydrothermal denaturation temperature (T_d). Three times were repeated for each kind of tanned sample.

Solid State NMR Analysis

The samples BEFORE hydrothermal denaturation were those hide powder sealed in bags after tanning, and the samples AFTER hydrothermal denaturation were those hide powder after DSC test. Solid state NMR analysis was performed on 11.7T Bruker Avance III-400.

Table I
 T_d of hide powder and aluminum, silicon and phosphorus tanned collagen

Samples	White hide powder	Aluminum-tanned hide powder	Silicon-tanned hide powder	Phosphorus-tanned hide powder
T_d (°C)	61.5	73.2	84.3	85.6

^{27}Al NMR Analysis

Take 10 mg of hide powder before and after hydrothermal denaturation, seal and label as Al-1 and Al-2 respectively. The test conditions were as below: 4 mm three resonance probe, rotation frequency 10 kHz, resonance frequency 130.4 MHz, single pulse sequence, pulse width 0.4 μs (ca. $\pi / 6$), relaxation time 1 second. The chemical shift of 1 mol/L $\text{Al}(\text{NO}_3)_3$ solution is referred to 0 ppm.

^{29}Si NMR Analysis

Take 10 mg of hide powder before and after hydrothermal denaturation, seal and label as Si-1 and Si-2 respectively. Test conditions were as below: using a 7 mm probe, the resonance frequencies of ^1H and ^{29}Si are 399.33 MHz and 79.33 MHz respectively. ^{29}Si MAS NMR single pulse sampling, $\pi / 2$ pulse is 6.0 μs , sampling delay is 60 s, rotational speed is 5 kHz, kaolin calibration (-91.5 ppm).

^{31}P NMR Analysis

Take 10 mg of hide powder before and after hydrothermal denaturation, seal them and label as P-1 and P-2 respectively. Test conditions were as below: resonance frequency 202.8 MHz; high energy decoupling, repetition time 4 s; pulse width 2 μs (ca. $\pi / 4$); 85% H_3PO_4 as reference sample. Other conditions are the same as ^{27}Al NMR analysis.

Results and Discussion

Results of DSC Analysis

The hydrothermal denaturation temperatures (T_d) of hide powder tanned with aluminum, silicon and phosphorus tanning agents from DSC analysis are listed in Table I.

Analysis of ^{27}Al NMR Result

It is known from previous work¹¹ that, when pH value is less than 2.5, there are few single Al^{3+} complexes in aluminum tanning solution, instead of that, aluminum ions will mainly form linear poly-ion complexes with 2~4 Al^{3+} (as shown in Fig. 1a); when pH value is about 4.0, spherical " Al_{13} " complexes with 13 Al^{3+} will be the main components (as shown in Figure 1b). The chemical shifts of linear polyion complexes with 2~4 Al^{3+} are in the range of 2~5 ppm, while the chemical shifts of spherical " Al_{13} " complexes are about 72 ppm. The chemical shifts of these two kinds of aluminum complexes are positively correlated with the number of Al^{3+} .¹¹

Figure 2 is the ^{27}Al NMR spectrum of collagen samples tanned with aluminum salt before and after hydrothermal denaturation. It can be obtained that, the chemical shifts of Al in the collagen samples tanned with aluminum salt before and after hydrothermal denaturation are 4.1 ppm and 2.9 ppm, respectively. Although

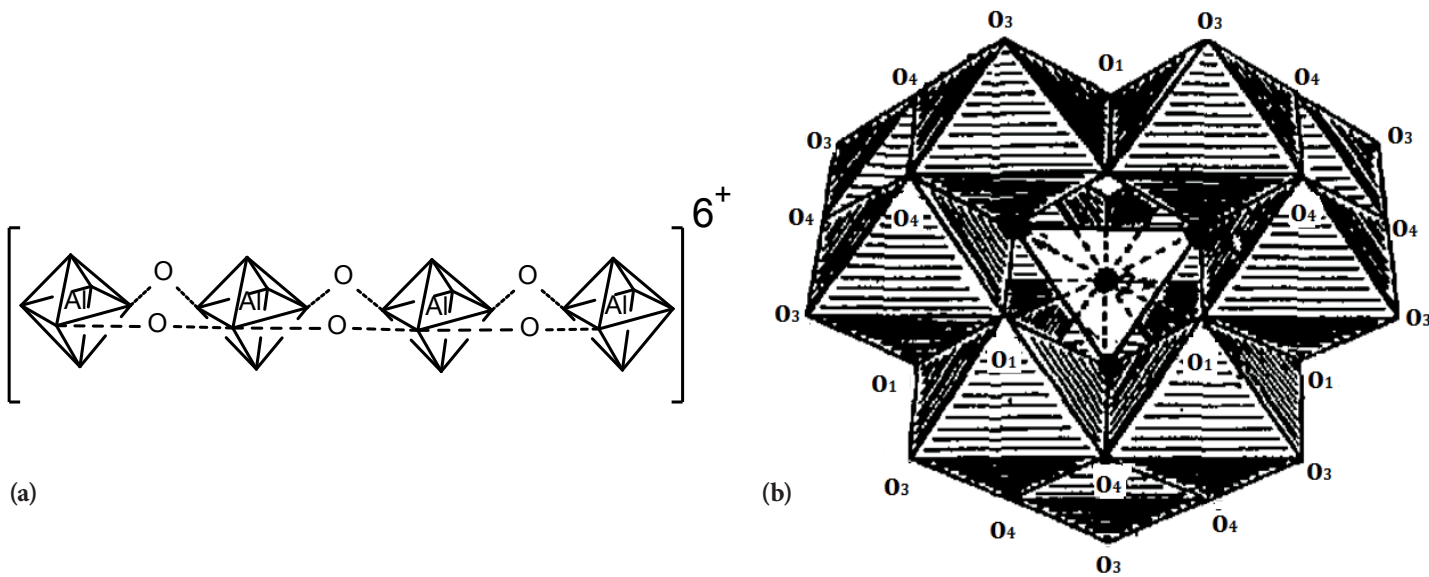


Figure 1. Structure of two kinds of aluminum complexes in tanning solution ((a) linear; (b) " Al_{13} ")

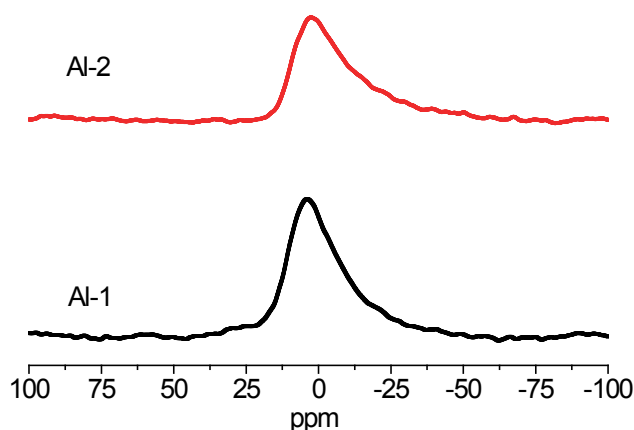


Figure 2. ^{27}Al NMR of aluminum-tanned collagen before and after denaturation (Al-1 —before denaturation, Al-2 —after denaturation)

the pH value of tanning solution is increased to above 4.5 in the later stage of aluminum tanning process, and at this pH value, the aluminum complexes in tanning solution should be spherical “ Al_{13} ” complexes theoretically.¹¹ However, it can be seen from Figure 2 that, both the aluminum complexes in hide powder before and after denaturation exist as linear polyion complexes with 2~4 Al^{3+} . In other words, there are no “ Al_{13} ” complexes in aluminum tanned hide powder. The possible inference for this fact is that, either “ Al_{13} ” complexes are too large to penetrate into collagen, or “ Al_{13} ” complexes are transformed into linear complexes with 2~4 Al^{3+} after hide powder leaving tanning solution. In a word, linear complexes composed of 2~4 Al^{3+} play the dominating role in tanning process.

It can also be seen from Figure 2 that the chemical shift of Al in aluminum tanned collagen hardly changes after denaturation (in ^{27}Al NMR spectrum, the small difference between 2.9 ppm and 4.1 ppm might be caused by the shielding effect of the conformational change on the central Al^{3+} ion caused by the hydrothermal denaturation of collagen). This result is consistent with that of Covington et al.¹⁰ The explanation given by Covington et al. is that there is no cross-linking between the aluminum complexes and the collagen side groups.

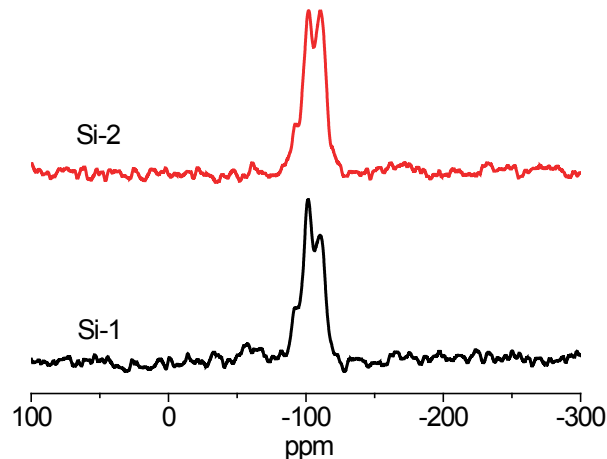


Figure 3. ^{29}Si NMR of silicon tanned hide powder before and after denaturation (Si-1 —before denaturation, Si-2 —after denaturation)

However, we speculated that, there might be another possibility, that is, after the hydrothermal denaturation of the collagen, the coordination bonds between the aluminum complexes and the collagen side groups are not broken.

Analysis of ^{29}Si NMR Results

Zhang et al.¹³ considered that silicic acid tanning agent mainly produced tanning effect on collagen through hydrogen bonds. It can be seen from Figure 3 that, both the chemical shift of Si in the collagen before and after hydrothermal denaturation is about -100 ppm. This result indicates that Si-O bonds and Si-Si bonds of silicon tanning agent in tanned collagen are not broken after hydrothermal denaturation. From this result, we could speculate that, the hydrothermal denaturation might be caused by the destruction of hydrogen bond among the tanned collagen molecules.

Analysis of ^{31}P NMR Results

Relevant studies suggest that the tanning mechanism of THPC is shown in Figure 4: each molecule of THPC contains four hydroxymethyl groups, which can form multi-point cross-linking with the amino groups of collagen molecules via covalent bonds.^{12,14}

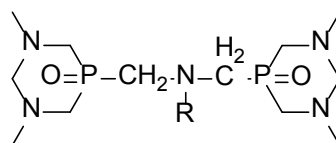
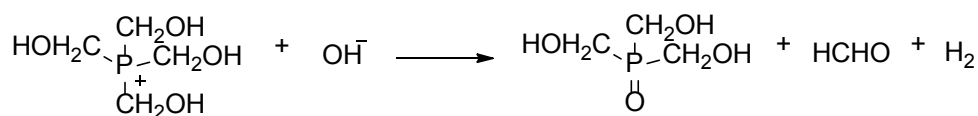


Figure 4. Tanning mechanism of THPC

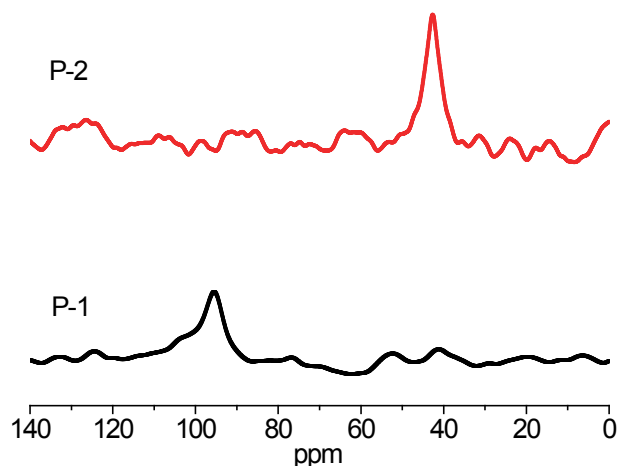


Figure 5. ^{31}P NMR of THPC tanned hide powder before and after denaturation (P-1—before denaturation, P-2—after denaturation)

It can be seen from Figure 5 that, the chemical shift of P in THPC tanned collagen is 95.5 ppm before hydrothermal denaturation, and it moves to 42.7 ppm after denaturation. Since the chemical shift of P in unreacted THPC is 26.5–27.2 ppm, Shao et al. speculated that the P-C bond of THPC was broken during the reaction with collagen, releasing formaldehyde, which was oxidized (as shown in Fig. 4), resulting in the chemical shift of P moving to 95.5 ppm in THPC tanned collagen.¹² Therefore, the results of ^{31}P NMR as shown in Figure 5 can be explained as follows: during the hydrothermal denaturation of collagen, a large number of amino, hydroxyl and carboxyl groups in collagen changed from ordered state to disordered state, which may form hydrogen bonds with oxygen atoms in P = O double bonds; or during the denaturation of collagen, P = O double bonds was reduced to P-O single bonds, resulting in the increase of electron cloud density around phosphorus atoms. Thus, the chemical shift moved to the high field. On the one hand, this result indicated the formation of covalent bonds between THPC and collagen molecules during the tanning process. On the other hand, the chemical bonds between THPC and collagen molecules were changed after hydrothermal denaturation, but they did not completely return to the state before tanning reaction. This conclusion could be deduced from the fact that, the chemical shift of P in denatured THPC tanned collagen was 42.7 ppm, while that in unreacted THPC is 26.5–27.2 ppm.

Conclusion

The chemical shifts of Al, Si and P in hide powder tanned with aluminum, silicon and phosphorus tanning agents before and after hydrothermal denaturation were analyzed by ^{27}Al NMR, ^{29}Si NMR and ^{31}P NMR. From the changes of their chemical shifts, following conclusions could be obtained:

- (1) Linear complexes composed of 2~4 Al^{3+} play the dominated role in aluminum tanning process. The chemical shift of

Al in the complexes reacted with collagen molecules by coordination bonds have no change (slightly moving to high field) after hydrothermal denaturation of collagen. Therefore, it can be speculated that either there are no coordination cross-linking between aluminum complexes and the side groups of collagen molecules, or the coordination cross-linking bonds between aluminum complexes and the side groups of collagen molecules are not broken after hydrothermal denaturation.

- (2) It can be inferred that Si-O and Si-Si bonds are not broken after hydrothermal denaturation of collagen, and the hydrothermal denaturation might be caused by the destruction of hydrogen bonds among the tanned collagen molecules.
- (3) The results show that the chemical shift of P moves to high field obviously after hydrothermal denaturation. It can be inferred that the covalent bonds between THPC and collagen molecules occur during tanning process. After hydrothermal denaturation, the chemical bonds between THPC and collagen molecules are partly broken, i.e., they do not completely return to the state before tanning reaction.

Acknowledgement

This work was financially supported by grants from the National Natural Sciences Foundation (No. 21776231) of China. Thanks to Professor Shen Wen-jie of Dalian Institute of Chemical Physics, Chinese Academy of Sciences for his support in solid state NMR testing.

References

1. Covington A. D.; Theory and mechanism of tanning: Present thinking and future implications for industry, *J. Soc. Leather Tech. Chem.*, **85**, 24-34 2001.
2. Brown E. M., Dudley R. L., Elsetinow A. R.; A conformational study of collagen as affected by tanning procedures, *JALCA* **92**, 225-233, 1997.
3. Ramasami T.; Approach towards a unified theory for tanning: Wilson's dream, *JALCA* **96**, 290-304, 2001.
4. Han W., Han G., Zhang M., et al. Reaction mechanism of organic tanning agents DC with skin collagen, *Leather Science and Engineering*, **30**(1), 33-36, 2020.
5. Zhang R., Wei D.; Study on Tanning Mechanism of Acrylic Polymer with X- ray Diffraction Method, *China Leather*, **28**(5), 6-10, 1999.
6. Zhang Q., Tang C., Ding K., et al.; Analysis for hydrogen bond changing of collagen by FT-IR and Raman spectrum, *China Leather*, **49**(1), 16-21, 2020.

7. Ding Y., Chen L., Li T.; Application of Molecular Simulation to Investigate Chrome (III) Crosslinked Collagen Problems, *Chinese Chemical Society*. Abstracts of the 29th Annual Conference of Chinese Chemical Society - 15th chapter, 2014.
 8. Li Y., Shao S., Shan Z. Tanning mechanism of THPC, *China Leather*, **19**, 15-18, 2005.
 9. Romer F. H., Underwood A. P., Senekal N. D., et al.; Tannin Fingerprinting in Vegetable Tanned Leather by Solid State NMR Spectroscopy and Comparison with Leathers Tanned by Other Processes, *Molecules*, **16**(2), 1240-1252, 2011.
 10. Covington A. D., Hancock R. A.; ^{27}Al NMR analysis on aluminum (III) tanned hide powder before and after shrinkage, *JSLTC*, **73**(1), 1-7, 1989.
 11. Ding Keyi; Study on the composition, structure and reactivity with collagen of organic acid masked aluminum complexes. *Doctoral Dissertation of Sichuan University*, 2001.
 12. Shao S., Shi K., Li Y., et al.; Mechanism of Chrome-free Tanning with Tetra-hydroxymethyl Phosphonium Chloride, *Chinese Journal of Chemical Engineering*, **16**(3), 446-450, 2008.
 13. Zhang Z., Liu J., Wang J., et al.; Insight into Understanding Incorporation of Glycidoxypropyltrimethoxysilane for Improving Hydrothermal Stability and Porous Structure of Silicic Acid Tanned Leather, *JALCA* **114**, 300-312, 2019.
 14. Matthews N. S., Lloyd G.R.; Use of phosphorous compounds in the production of leather. *Journal of Cleaner Production*, **87**, 39-49, 1993.
-

Fabrication of Composite Films Based on Chitosan and Vegetable-Tanned Collagen Fibers Crosslinked with Genipin

by

Jie Liu,^{a†} Yanchun Liu,^a Eleanor M. Brown,^b Zhengxin Ma,^a and Cheng-Kung Liu^{b†}

^a*School of Materials Science and Engineering, Zhengzhou University, Zhengzhou, Henan 450001, China*

^b*Eastern Regional Research Center, United States Department of Agriculture,* Wyndmoor, PA 19038, USA*

Abstract

The leather industry generates considerable amounts of solid waste and raises many environmental concerns during its disposal. The presence of collagen in these wastes provides a potential protein source for the fabrication of bio-based value-added products. Herein, a novel composite film was fabricated by incorporating vegetable-tanned collagen fiber (VCF), a mechanically ground powder-like leather waste, into a chitosan matrix and crosslinked with genipin. The obtained composite film showed a compact structure and the hydrogen bonding interactions were confirmed by FTIR analysis, indicating a good compatibility between chitosan and VCF. The optical properties, water absorption capacity, thermal stability, water vapor permeability and mechanical properties of the composite films were characterized. The incorporation of VCF into chitosan led to significant decreases in opacity and solubility of the films. At the same time, the mechanical properties, water vapor permeability and thermal stability of the films were improved. The composite film exhibited antibacterial activity against food-borne pathogens. Results from this research indicated the potential of the genipin-crosslinked chitosan/VCF composites for applications in antimicrobial packaging.

Introduction

The utilization of polymer matrices for packaging applications has attracted intense scientific and practical interests because of the outstanding physical properties and versatile processibility arising from their aggregation structure. At present, though petroleum-based, non-degradable thermoplastics are used worldwide for packaging applications and will still play an important role in the foreseeable future, many countries and districts are paying more attention to the development and use of biodegradable bio-based polymers in packaging materials.¹ Moreover, the rapidly growing demand for antimicrobial packaging materials leads to a strong interest in blends and films to suppress the growth and accumulation of harmful bacteria.^{2,3} As a unique biodegradable cationic linear polysaccharide extracted from marine sources, chitosan consists of β -1,4-linked glucosamine and N-acetyl-D-glucosamine. Due to

this unique chemical structure, chitosan is known to have intrinsic antimicrobial activity against bacteria, yeasts, molds and fungi.⁴ It also has excellent biocompatibility, nontoxicity and physical stability. Because of these beneficial properties, chitosan is widely used in biomedical, packaging, pharmaceutical, food and environmental applications.⁵

Collagen is the most abundant protein in animal tissues. It is in the form of a long, highly ordered, triple-helical fibrillar structure.⁶ As by-products of the meat industry, animal hides, skins and bones are principal sources of collagen. Though collagen finds a variety of applications in the food industry, tissue engineering, wound dressing and drug delivery due to its excellent biocompatibility and safety, huge amounts of raw hide and skin are sent to tanneries in order to transform them into luxury and precious leather.^{7,8} The production of leather can be accomplished using different kinds of tanning agents that stabilize the collagen matrices. Vegetable tanning is one of the oldest leather-making technologies, which uses mainly phenolic compounds present in leaves, barks, roots, wood or galls of many plants to produce eco-friendly durable leather.⁹ Until now, vegetable-tanned leather is still widely used for the production of footwear, bookbinding, harnesses, belts, and upholstery. During the leather-making process, however, a huge amount of leather waste comprised of crosslinked collagen fibers is generated and discarded. It has been estimated that approximately 200 kg of tanned and 250 kg of un-tanned solid waste may be generated and discarded when one ton of raw hide is processed.⁷ The solid leather waste includes trimmings, shavings, fleshings, buffing dusts, etc. Statistical data reveals that nearly 1.4 million tons of leather solid waste is produced annually in China.¹⁰ In addition to the environmental problems, the arbitrary disposal of these collagen-containing leftovers represents a waste of a valuable protein resource. In order to make the best use of these proteins, great effort and comprehensive studies on converting leather waste into value-added products have been performed over the past decades.¹¹

Since collagen fibers can be physically de-bundled and refined from leather solid waste by mechanical grinding, a promising strategy for reclamation of these protein wastes is to incorporate leather fibers into polymer matrices for various applications, such as packaging,

*Mention of trade names or commercial products in this article is solely for the purpose of providing specific information and does not imply recommendation or endorsement by the U.S. Department of Agriculture (USDA). USDA is an equal opportunity provider and employer.

†Corresponding author emails: liujie@zzu.edu.cn, chengkung.liu@usda.gov

Manuscript received March 2, 2021, accepted for publication May 6, 2021.

building materials, footwear, and clothing.¹²⁻¹⁴ A lot of work has been done by researchers to develop novel bio-based composites from blends of leather fibers and cellulose, cellulose derivatives, natural rubber latex, etc.^{15,16} In our previous studies, vegetable-tanned leather fibers have been incorporated into a gelatin matrix using a paper-making procedure and casting method to develop novel composite materials for packaging applications.^{13,14} These composites exhibited better mechanical and thermal properties and may be used as a raw material for the preparation of consumer products. In addition to the bio-based polymer matrices, leather fibers have also been incorporated into different kinds of petroleum-based thermoplastic polymers, such as polyurethane,¹² natural rubber,¹⁷ polyvinyl alcohol,¹⁸ polylactic acid,¹⁹ etc. These research projects offer various potential solutions for reducing environmental pollution caused by tannery waste, as well as provide new ways for the fabrication of low-cost eco-friendly composite materials.

Though several studies have been done on collagen fiber reinforced/filled composites with different polymers, very few are with chitosan. In the present work, collagen fibers from vegetable-tanned leather waste were prepared by grinding. Then, a series of chitosan/vegetable-tanned collagen fiber (VCF) composite films with varying weight percentage of VCF (from 5.0 to 25.0 wt%) were prepared. A naturally occurring crosslinking substance with low toxicity, genipin, was used to crosslink the chitosan matrix. The structure, optical property, water absorption property, water vapor barrier property, thermal stability and mechanical properties of the crosslinked chitosan/VCF composite films were investigated. Moreover, the antibacterial activity of the composite film against Gram-positive and Gram-negative bacteria were assessed using an agar diffusion method.

Experimental

Materials

Chitosan (molecular weight 50-190 KDa, degree of deacetylation 75-85%), acetic acid and glycerol were obtained from Sigma-Aldrich Chemical Co., USA. Genipin was provided by Challenge Bioproducts Co. Ltd., Taiwan. Vegetable-tanned bovine split samples were obtained from a local vegetable tannery (Wicket and Craig, Curwensville, PA, USA). The leather scraps were cut into small pieces (2.5-5.5 cm²) and dried. Then, the leather pieces were ground in a Model 4 Wiley Mill (Thomas Scientific, USA) to pass through a 2-mm screen. The obtained collagen fibers were collected and sealed in plastic bags at ambient temperature (22-25°C).

Characterization of VCF

The digital optical micrograph of VCF was obtained using a 59XC-PC polarized optical microscope (Shanghai Optical Instrument Factory, China). Differential scanning calorimetry (DSC) analysis

was carried out using a multi-cell DSC analyzer (TA Instruments, USA) to detect the denaturation behavior of collagen fibers under nitrogen flow. The elemental analysis was performed using a Vario Micro Cube elemental analyzer (Elementar, Germany) to quantify the content of C, H, N, and S in VCF.

Preparation of films

Chitosan (CS) and genipin-crosslinked chitosan/VCF (G-CS/VCF) films were prepared using a solvent casting method. CS powder was dispersed in 1% (v/v) acetic acid aqueous solution to obtain a transparent CS solution (1%, w/v) while mixing vigorously at room temperature ($\approx 25^\circ\text{C}$). Then, vegetable-tanned leather fiber (5%, w/w based on chitosan) was added to the CS solution. Glycerol (40%, w/w based on chitosan) was used as a plasticizer to improve the flexibility of the resulting films. After 30 min of mixing, 10 mL of genipin aqueous solution in a concentration of 10 mg/mL was added to 100 mL of the chitosan/VCF mixture. After thoroughly stirring and vacuum degassing, the obtained solution was poured into plastic Petri dishes and allowed to dry at 50°C for 24 h. The as-prepared films were peeled off from the casting surface and placed in a vacuum chamber for 2 h at 80°C to further remove the acetic acid residue. The films were stored over silica gel before characterization. The procedure was repeated to prepare a series of films containing 10.0, 15.0, 20.0 and 25.0 wt% (based on chitosan) of VCF. The genipin-crosslinked chitosan/VCF films containing 5.0, 10.0, 15.0, 20.0 and 25.0 wt% (based on chitosan) of VCF were denoted as G-CS/VCF5, G-CS/VCF10, G-CS/VCF15, G-CS/VCF20 and G-CS/VCF25, respectively. Chitosan film prepared from pure chitosan with genipin crosslinking (G-CS) was prepared as a control. Prior to moisture content tests and mechanical properties studies, film samples were conditioned in a constant temperature and humidity chamber at $24 \pm 1^\circ\text{C}$ and 50% relative humidity (RH) for 7 days. The thicknesses of the films were measured to be in the range of 0.15-0.25 mm using a Palmer digital micrometer (Comecta, Spain).

Characterization of the films

Fourier transform infrared analysis

Fourier transform infrared (FTIR) spectra of the chitosan-based films were collected using a Nicolet 6700 spectrophotometer (Thermo Fisher Scientific, USA). An attenuated total reflection (ATR) accessory was applied during the process. Each spectrum was obtained with 60 scans per sample ranging from 500-4000 cm⁻¹.

X-ray diffraction analysis

The X-ray diffraction (XRD) patterns were recorded on an Empyrean X-ray diffractometer (PANalytical, Netherlands) equipped with a Cu K α radiation source ($\lambda=0.1546\text{nm}$), at operating voltage and current of 40 kV and 30 mA, respectively. Measurements were performed in the range of 10°-60° (2 θ), and the step-size was 0.02°.

Scanning electron microscopy

Morphology of the film samples was observed by scanning electron microscopy (SEM) using a Model JSM 840A scanning electron microscope (JEOL, USA). The films were fractured in liquid nitrogen so as to expose the cross sections. The samples were fixed on specimen stubs using Duco cement. All samples were sputter-coated with an ultrathin layer of gold to permit the observation of their microstructure. All samples were examined with an accelerating voltage of 10 kV.

Optical properties

The optical barrier properties of the films were measured according to ASTM D1746-09 method with slight modifications.²⁰ The transmission measurements were performed using a UV-Vis spectrophotometer (Cary 50, Agilent, USA) at the ultraviolet (UV) and visible range (200-800 nm).

The color difference between films were determined using a digital colorimeter (JZ-300, Shenzhen Kingwell Instrument Co., Ltd, China). CIELAB color parameters L^* (represent lightness), a^* (represent red/green) and b^* (represent yellow/blue) of the films were recorded. All colorimetric measurements were performed on a white board as standard background. The values of color parameters of the white standard were determined to be: $L^* = 93.58$, $a^* = 1.54$, and $b^* = -0.50$. The values of total color difference (ΔE^*) can be calculated according to the following equation:

$$\Delta E^* = \sqrt{(\Delta L^*)^2 + (\Delta a^*)^2 + (\Delta b^*)^2} \quad (1)$$

where ΔL^* , Δa^* , and Δb^* represent the differences between parameters L^* , a^* , and b^* of the film samples and those of the white standard, respectively. Films were analyzed in triplicate, recording five measurements for each sample.

Moisture content and water solubility

After preconditioning as mentioned above, the moisture content (MC) of the films was determined using a moisture analyzer (MF-50, A&D Company, Japan). Films were spread on the pan and heated at 130°C for 10 min. The MC value was calculated based on the following formula:

$$MC(\%) = \frac{(m_i - m_d)}{m_d} \times 100 \quad (2)$$

where m_i and m_d denote the initial and dried weights of the film sample, respectively. Afterwards, the dried samples were soaked in 30 mL of 50 mM PBS solution (pH 7.4) for 24 h at 25°C. Finally, the swollen films were removed from the PBS, and their surfaces were blotted with filter papers. The films were placed in the moisture analyzer again to evaporate excess water at 130°C. Total soluble matter (TSM) was calculated by the following equation:

$$TSM(\%) = \frac{(m_d - m_f)}{m_f} \times 100 \quad (3)$$

where m_f is the weight of the remnant dry matter.

Water vapor permeability

Water vapor permeability (WVP) of the films was measured at 20°C according to ASTM E96-00 with slight modifications.²¹ Glass gas permeation bottles (diameter 15 mm, height 45 mm) containing distilled water (100% RH). The film sample was tightly sealed on top of the permeation bottle and the headspace for the bottle was 1.0 cm from the opening of the bottle. The bottle was placed in a desiccator containing 200 g fully dried silica gel (0% RH). The weight of the bottle was measured at 24-hour intervals over a period of 7 days. Then the weight values of the bottle were plotted against time and the slope of the linear regression lines were calculated. The value of WVP was obtained according to the following equation:

$$WVP = \frac{(WVTR \times L)}{\Delta P} \quad (4)$$

where WVTR is water vapor transmission rate (the slope of weight vs. time divided by the permeation area of film); L is the mean thickness of film; ΔP denotes the partial water vapor pressure difference across the two sides of the film.

Thermogravimetric analysis (TGA)

The thermal degradation behavior of the films was analyzed using a Q500 thermogravimetric analyzer (TA Instruments, USA) in 20-800°C temperature range under nitrogen atmosphere with a purge gas flow of 60 mL/min. Approximately 6-8 mg of the sample was used for each test. The temperature was increased at a heating rate of 10°C/min.

Mechanical properties

Tensile strength (TS), Young's modulus (YM) and elongation at break (EAB) of the films were measured using an Insight 5 mechanical property tester (MTS Systems, USA). The specimens were in rectangular shape with dimension of 50 mm × 5 mm. After conditioning at 24 ± 1°C and 50% RH for 7 days, tensile tests were performed at approximately 24°C and 50% RH. The initial grip separation was 25 mm and the grips were separated at a rate of 50 mm/min. For each film, five specimens were tested to obtain a representative value.

Dynamic mechanical analysis

The dynamic mechanical properties of the chitosan-based films were tested using a Q800 dynamic mechanical analyzer (TA instruments, USA) under tensile mode. Rectangular specimens (50 mm × 5 mm) were equilibrated at 24 ± 1°C and 50% RH for 7 days. Each measurement was conducted at a heating rate of 2°C/min in the temperature range of 20-220°C, with an amplitude of 10 μm at a frequency of 1 Hz.

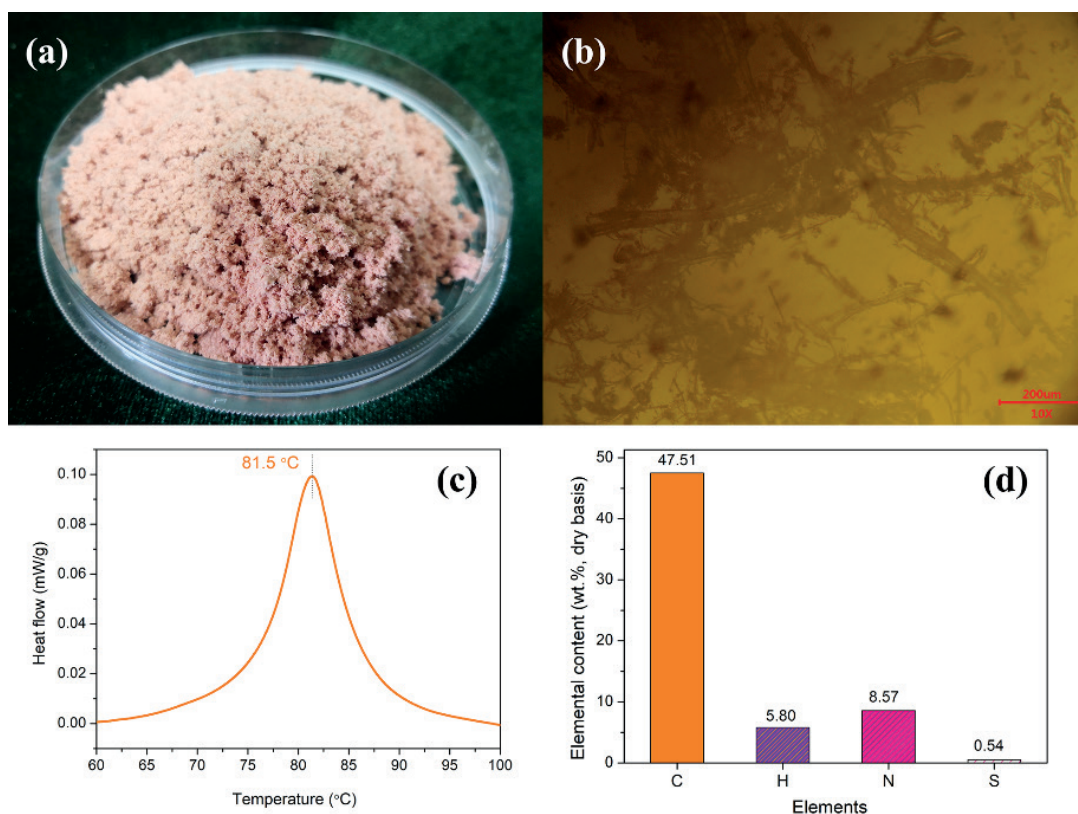


Figure 1. (a) Appearance, (b) optical micrograph, (c) DSC curve and (d) elemental analysis results of the VCF.

Antibacterial activity

The antibacterial activity of the film was assessed using the disc-diffusion method against two foodborne bacterial pathogens: *E. coli* (Gram-negative) and *S. aureus* (Gram-positive). Films were cut into small discs (8 mm in diameter) and placed on agar plates, which had been previously seeded with 100 μ L of bacterial solution. The bacteria were cultured in an incubator at $37 \pm 0.5^\circ\text{C}$ for 24 h. The antibacterial effectiveness was evaluated by observing the presence or absence of a zone of inhibition around the sample disc.

Results and discussion

Characterization of VCF

Figure 1 shows the appearance, optical micrograph, DSC curve and elemental analysis results of the VCF obtained from the vegetable-tanned leather. The visual appearance of the VCF sample is quite similar to the visual appearance of other hide powders, but with a characteristic light brown color originated from the vegetable tannins (Figure 1a). According to the observation of optical micrograph (Figure 1b), the fibers show obvious variations in their sizes and shapes. Figure 1c shows the typical DSC curve of the hydrated VCF sample in a sealed crucible. There is a distinct endotherm peak at 81.5°C on the curve, corresponding to the thermal denaturation and shrinkage of collagen fibers. Elemental analysis confirmed

large amounts of carbon and nitrogen in the sample, which are in accordance with the results for vegetable-tanned shavings reported by Yilmaz et al.²²

Structural characterization of the films

FTIR is useful for obtaining information about the molecular structure of biopolymers. Figure 2 shows the FTIR spectra of the chitosan-based films. For neat CS, the broad band ranging between 3000 and 3600 cm^{-1} is assigned to the O-H stretching vibration, and it also overlaps with the N-H band asymmetric/symmetric stretching vibration. The bands at 1639, 1545 and 1323 cm^{-1} are attributed to the Amide I (C=O stretching), Amide II (N-H bending), and Amide III (C-N stretching) modes, respectively.²³ The bands at 1152 and 924 cm^{-1} are characteristic of its saccharide structure.²⁴ Compared to the FTIR spectra of neat CS, the peak intensity of 1151 cm^{-1} , corresponding to asymmetric C-O-C stretching and C-N stretching, are slightly increased at the expense of decreasing peak intensity of band at 1025 cm^{-1} (skeletal vibration of the C-O stretching).²⁵ This could be attributed to the formation of additional C-N bonds during the crosslinking reaction, according to the mechanism of crosslinking of chitosan by genipin.²⁶ Some differences can be found after VCF addition into the G-CS matrix. The band between 3000 and 3600 cm^{-1} becomes broader and the peak shifts from 3272 to 3268 cm^{-1} as a result of the addition of VCF, suggesting an increase in hydrogen bonding interactions between CS and VCF. Similar

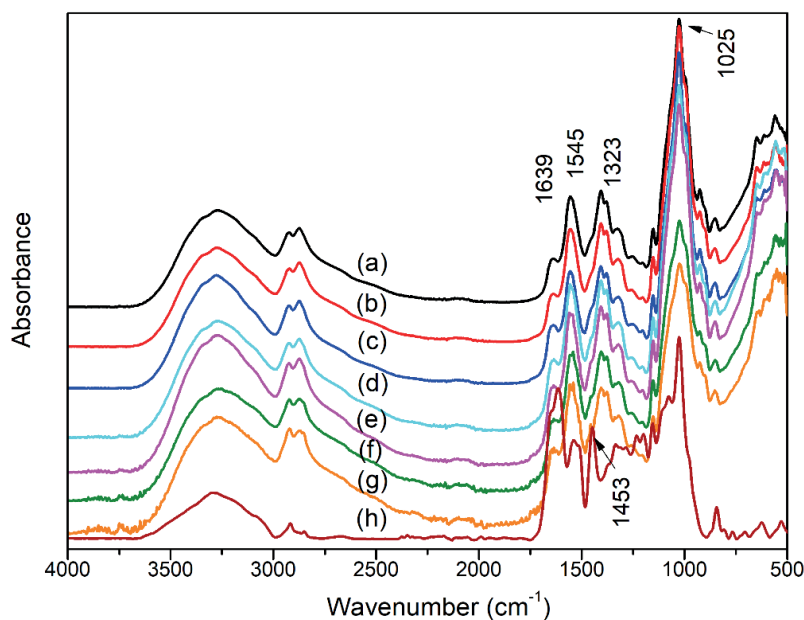


Figure 2. ATR-FTIR spectra of (a) neat CS, (b) G-CS, (c) G-CS/VCF5, (d) G-CS/VCF10, (e) G-CS/VCF15, (f) G-CS/VCF20, (g) G-CS/VCF25 films and (h) VCF.

spectral changes have been reported for other chitosan-based composite materials.²⁷ Moreover, a small shoulder peak appears at 1453 cm^{-1} (aromatic ring stretch vibration), indicating the presence of vegetable tannins present in the films.²⁸

The XRD patterns of the genipin crosslinked chitosan-based films are shown in Figure 3. Chitosan is semi-crystalline in nature. However, after making the genipin crosslinked films, the chitosan-based films exhibit only one main broad diffraction peak at $2\theta = 20.5^\circ$, corresponding to the amorphous state of chitosan. The incorporation of VCF did not produce new peaks with respect to G-CS film, and no significant shift in the diffraction peak was

observed. Although previous research on crystalline structures of pure chitosan have identified a diffraction peak at $2\theta = 10\sim 12^\circ$, corresponding to the hydrated semi-crystalline structure, this peak was almost indiscernible in this study.²⁹ This could be due to the formation of covalent crosslinks through genipin bridges between chitosan molecular chains in which the strong interaction restricts the movement of the chitosan chains and suppresses its crystallization. Another possible reason is the presence of amorphous VCF retards the crystal growth of the chitosan matrix. Joseph et al. also observed a decrease of crystallinity of polycaprolactone with the addition of waste leather buff.³⁰

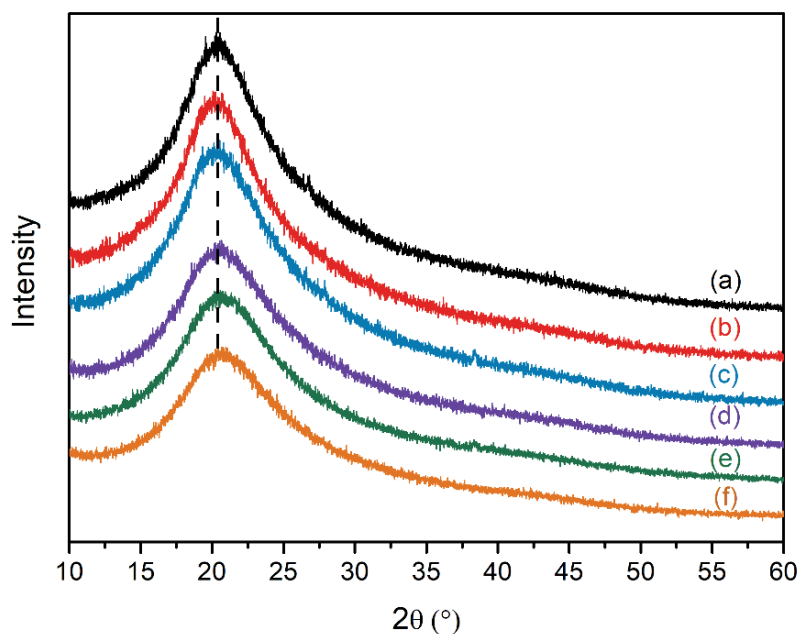


Figure 3. XRD patterns of (a) G-CS, (b) G-CS/VCF5, (c) G-CS/VCF10, (d) G-CS/VCF15, (e) G-CS/VCF20, and (f) G-CS/VCF25 films.

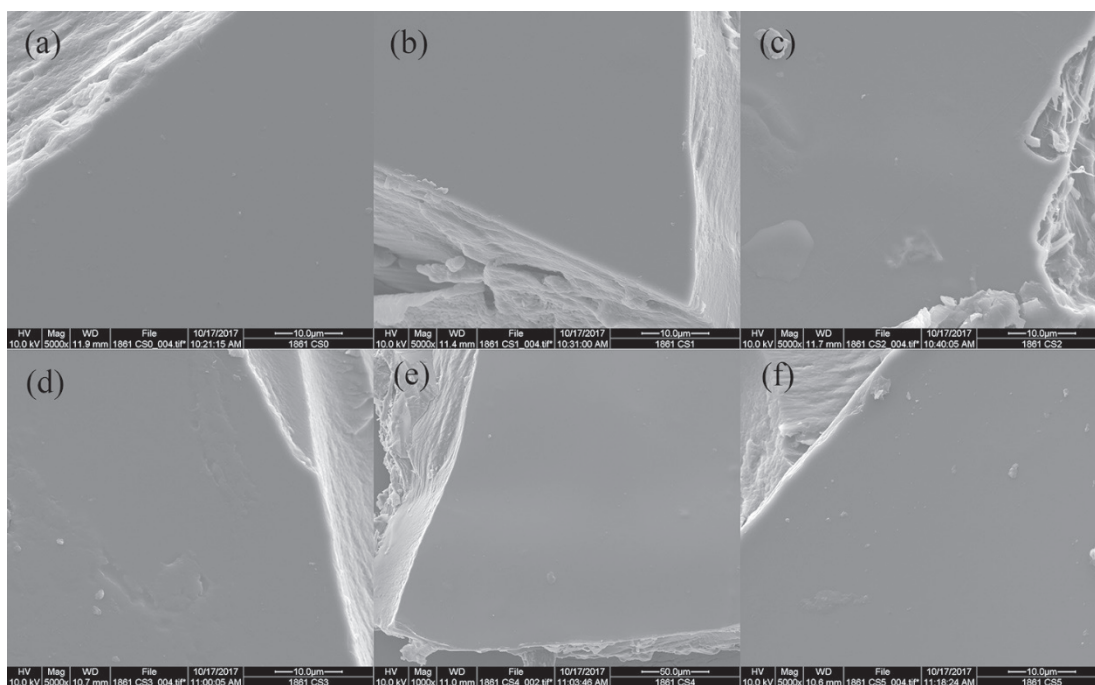


Figure 4. SEM images of the chitosan-based films. (a) G-CS; (b) G-CS/VCF5; (c) G-CS/VCF10; (d) G-CS/VCF15; (e) G-CS/VCF20; (f) G-CS/VCF25.

Figure 4 shows the surface and cross-sectional morphologies of G-CS and G-CS/VCF composite films. As can be seen, all films exhibit relatively smooth surfaces without obvious cracks and pores. The G-CS film has the most smooth and compact surface as expected (Figure 4a), while the addition of VCF caused slight changes in the surface microstructure (Figures 4b-f). From the broken side surface of the films, embedded collagen fibers can be observed in the chitosan matrix and there is little evidence of fiber pull-out, indicating that the interaction between vegetable-tanned leather fibers and chitosan is strong. SEM observations also

show that the leather fibers are morphologically different in the composite films, including single collagen fibers and collagen fiber bundles. The diameter of these fibers and bundles can be varied from nanometers to micrometers. Similar microstructures have been reported by Ambrósio et al. who worked with PVB/leather fiber composites.³¹

Optical properties

Figure 5 shows the transmittance spectra of the films in the UV and visible light range. All the genipin-crosslinked films transmission in

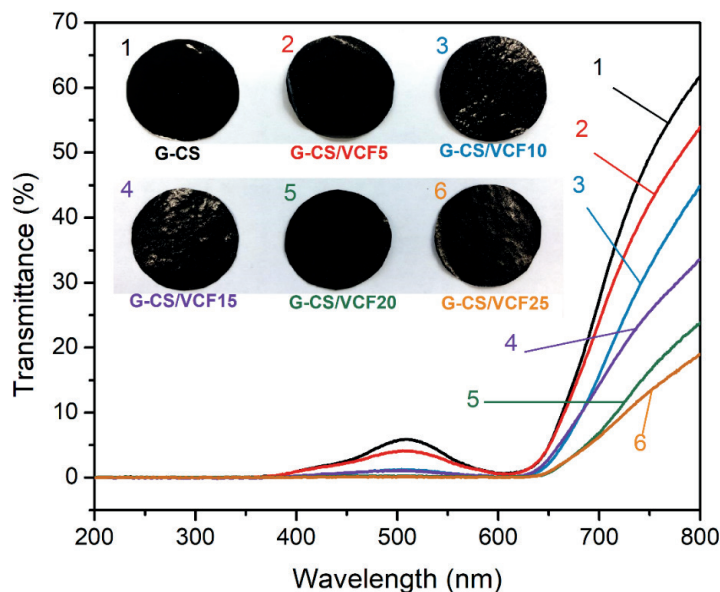


Figure 5. UV-Vis spectra of the genipin-crosslinked chitosan and chitosan/VCF composite films. The inset shows the digital images of the films.

Table I
Color parameters of the genipin-crosslinked chitosan-based films.

Samples	L*	a*	b*	ΔE^*
G-CS	16.91 ± 1.11 ^d	28.74 ± 2.80 ^a	-6.59 ± 0.66 ^d	81.62 ± 0.25 ^a
G-CS/VCF5	20.35 ± 0.82 ^c	21.77 ± 3.18 ^b	-6.32 ± 0.57 ^d	76.24 ± 0.98 ^b
G-CS/VCF10	23.53 ± 0.72 ^b	15.49 ± 0.60 ^c	-4.82 ± 0.44 ^c	71.55 ± 0.61 ^c
G-CS/VCF15	25.44 ± 0.67 ^{ab}	12.74 ± 0.85 ^{cd}	-3.82 ± 0.50 ^b	69.14 ± 0.58 ^{cd}
G-CS/VCF20	27.05 ± 0.6 ^a	10.45 ± 1.15 ^d	-3.39 ± 0.40 ^{ab}	67.20 ± 0.63 ^{de}
G-CS/VCF25	27.79 ± 2.99 ^a	8.30 ± 2.66 ^e	-2.71 ± 0.42 ^a	66.20 ± 3.28 ^e

Values are given as mean ± standard deviation. Different superscript letters in the same column indicate significant differences (a>b>c>d>e; $p < 0.05$).

the UV range are approaching the zero value, indicating excellent UV barrier properties of the films. This has been related to the generation of blue pigments via the reaction of genipin with chitosan and VCF in the presence of oxygen, which help to enhance the UV light absorbance of the film.^{32,33} This result is in agreement with previous reports that the genipin-chitosan mixture displays an increase in the intensity of the peaks at 240 nm and 280 nm from the start of the crosslinking reaction.³³ A transmittance peak was observed at a wavelength around 500 nm because of the formation of dark blue pigments during the crosslinking reaction. The blue color is presumed to be formed through oxygen radical-induced polymerization and dehydrogenation of the intermediate genipin compounds. According to the literature, the blue color is highly stable to heat, light and pH.^{33,34} Therefore, the blue pigments formed inside the polymer matrix would endow the composite film with high color stability, which is important for packaging applications. Furthermore, an increase of VCF content leads to an improvement of the film barrier to light. This can be ascribed to the hindrance effect of leather fibers on the passage of light. It is well known that packaging films that prohibit UV light passing through are very useful in inhibiting lipid oxidation in food and pharmaceutical systems.³⁵ Thus, G-CS/VCF composite film's low UV-visible transmittance makes it an ideal food and pharmaceutical packaging material for light-sensitive products.

Color is an important property for films because potential packaging applications may require different film appearances. As shown inside Figure 5, the genipin crosslinked films show an evident dark blue color, and the collagen fibers are evenly distributed within the dark blue chitosan phase. The films color measurement data are shown in

Table I. The incorporation of VCF into the genipin-crosslinked CS matrix led to an increase of L* ($p < 0.05$), indicating an increase in the lightness of the film. The decrease of a* indicates an intensification of greenness in the chitosan films ($p < 0.05$). Negative values of b* suggest the films have a blue tint. As the VCF content in the films increased the b* values increased as well (Table I). The total color difference (ΔE^*) can be utilized to evaluate how far apart two films are in the color space. It can be seen from Table I that the ΔE^* value of the composite films decreases gradually with increasing VCF content, in which the lower ΔE^* indicates a less colored film. The ΔE^* values obtained in the present study were higher than chitosan/gelatin composite films, but were comparable to genipin-crosslinked gelatin-based composite films.^{14, 36}

Moisture content and water solubility

Water absorbing capacity of polymers is strongly dependent on the amount of hydrophilic groups such as -NH₂, -OH, -CONH₂, etc.³⁷ Moisture content (MC) is related to the void volume that can be occupied by water in the matrix structure of the material. Figure 6 shows the MC results of G-CS and G-CS/VCF films having different contents of VCF. At lower VCF content (<15.0 wt%), the MC values of CS/VCF films are not significantly different ($p > 0.05$). However, increasing the weight percentage of VCF to 25.0 wt%, the MC values decreased from 19.5% to 15.8%. This may be attributed to the original void volume of the CS matrix is occupied by the leather fibers during the composite fabrication process. It was determined that fibrous leather has a lower MC value (13.5%) than that of the original genipin-crosslinked chitosan matrix (19.7%). As a result, the moisture content of composite films tended to decrease with an increase in leather fiber content.

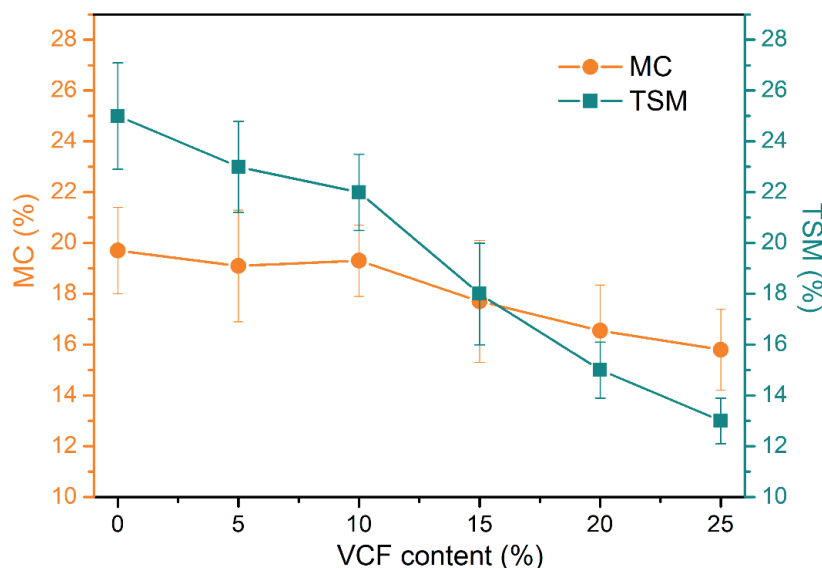


Figure 6. The effect of VCF content on moisture content (MC) and total soluble matter (TSM) of the genipin-crosslinked chitosan and chitosan/VCF composite films.

Total soluble matter (TSM) reflects the stability of a polymer film in water/aqueous medium, and a lower TSM implies higher stability in an aqueous medium. The TSM of the films with different VCF loadings are also shown in Figure 6. The TSM values are 25.0%, 22.9%, 22.4%, 17.7%, 14.9% and 12.8% for G-CS, G-CS/VCF5, G-CS/VCF10, G-CS/VCF15, G-CS/VCF20 and G-CS/VCF25, respectively. Results indicated that the addition of VCF led to a significant increase in stability of the chitosan-based films in aqueous solution. This property is of great importance to the packaging applications of such materials because it is closely related to their stability during production, storage and while in service.³⁸ The TSM values of the glycerol plasticized films obtained in this study were higher than those reported by Jin et al. for films made with blends of genipin-crosslinked chitosan and poly (ethylene oxide), possibly due to the difference in molecular weight and structure of the plasticizers.³⁹

Water vapor permeability

Water vapor permeability (WVP) values of the films are shown in Figure 7. For the chitosan film without VCF, the WVP was $0.86 \text{ g mm}^{-2} \text{ h}^{-1} \text{ kPa}^{-1}$, which was consistent with the results reported by Leceta et al.⁴⁰ With an increase of VCF weight percentage from 0 to 25.0 wt%, there is a clear trend of increasing WVP, indicating that the incorporation of leather fiber into the chitosan film affected the moisture transfer of the resulting films. It has been reported that the WVP values of films are affected by various factors, including the aggregation structure and hydrophilicity of the fiber and film matrix.⁴⁰ All these factors influence the solubility and diffusivity of water molecules in the film. Vegetable tannins are amphipathic molecules having a large number of free hydroxyl groups, which react with collagen primarily via hydrogen bonding. Hence, VCF is water-insoluble but is highly hydrophilic due to its polarity owing

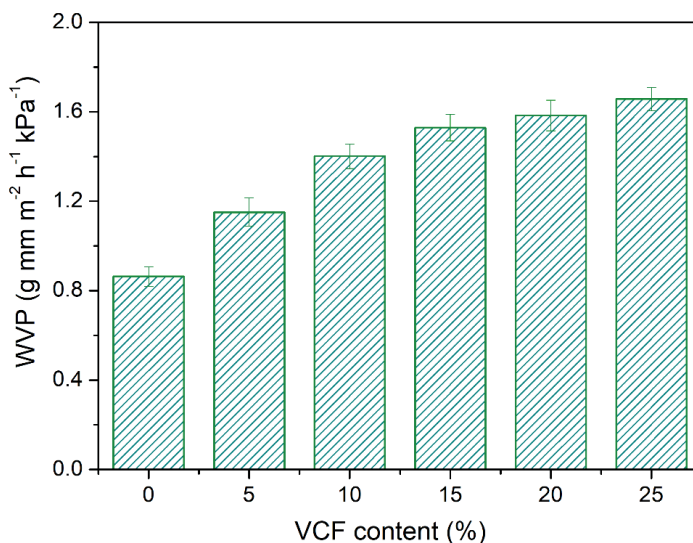


Figure 7. Water vapor permeability of the genipin-crosslinked chitosan and chitosan/VCF composite films.

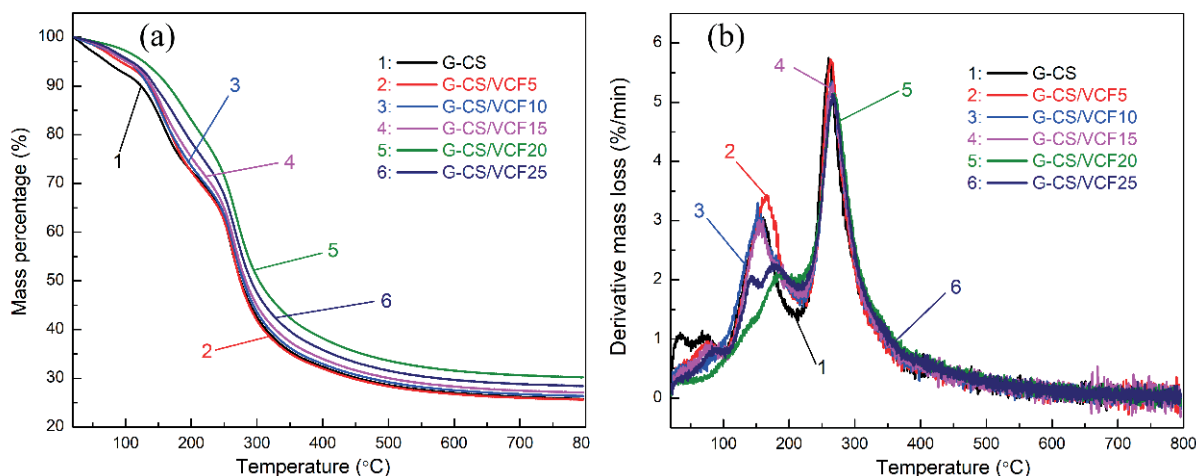


Figure 8. (a) TG and (b) DTG curves of the genipin-crosslinked chitosan and chitosan/VCF composite films.

to various hydrophilic groups from collagen and tannins. These fibers may raise the availability of the hydrophilic groups in the composite films and increase their interactions with water. In this regard, though the MC values of the composite films decreased with the addition of VCF (Figure 6), the high hydrophilicity and possible agglomeration of VCF may be responsible for the increase in WVP with the increase of VCF content. These two factors affect the transmission of water vapor through the composite films by forming a shorter path.

Thermal stability

Since packaging films may be submitted to heat treatment during fabrication, processing and application, thermal stability is an important property for these films. The thermal degradation behavior of the chitosan-based films was investigated by TGA. The TG/DTG curves obtained for all of the films are shown in Figure 8. Several stages of degradation are distinguished from the curves. The first weight loss stage observed in the temperature range 20-120°C is attributed to the release of moisture from the films (Figure 8(a)). In Figure 8(b), at least two distinct DTG peaks can be observed in the temperature range of 120-450°C, indicating that the thermal

degradation processes operate through different mechanisms. This stage can be assigned to the release of bound water and decomposition of the chitosan and collagen, along with the deacetylation of chitosan. Our previous study has shown that the main decomposition process of VCF was observed in the temperature range from 150 to 600°C.⁴¹ It has been reported that the residue of HAc in chitosan strongly influences the thermal degradation behavior of the matrix, which may induce enhanced degradation of chitosan at lower temperatures.⁴² Similar thermal degradation behaviors of chitosan and its composites were also observed by Wang et al.⁴³ The last thermal degradation stage, in the temperature range 450-800°C, can be associated with the degradation of the polymer chains (chitosan and collagen) of higher molecular weight and restructuring of the char formed during the former stages.⁴¹

Several TGA analytical parameters have been considered including: the decomposition temperature for 20% and 50% mass loss, denoted as $T_{20\%}$ and $T_{50\%}$, respectively; the temperature of the maximum rate of degradation as the decomposition temperature (T_{max}); and the solid residues remain at 600°C. The results are given in Table II. The $T_{20\%}$ and T_{max} of G-CS film were 164°C and

Table II
TGA parameters of the genipin-crosslinked chitosan-based films.

Sample	$T_{20\%}$ (°C)	$T_{50\%}$ (°C)	T_{max} (°C)	$R_{600^\circ\text{C}}$ (%)
G-CS	164	275	260	27.0
G-CS/VCF5	170	274	263	26.8
G-CS/VCF10	171	279	265	27.6
G-CS/VCF15	178	283	267	28.3
G-CS/VCF20	215	303	269	31.6
G-CS/VCF25	193	291	267	29.7

Table III
Mechanical properties of the genipin-crosslinked chitosan-based films.

Samples	Tensile strength (MPa)	Young's modulus (GPa)	Elongation at break (%)
G-CS	23.2 ± 1.0 ^b	0.98 ± 0.32 ^a	8.6 ± 0.3 ^e
G-CS/VCF5	23.8 ± 1.1 ^{ab}	0.67 ± 0.11 ^{cd}	9.1 ± 0.3 ^{de}
G-CS/VCF10	25.5 ± 1.6 ^a	0.76 ± 0.18 ^c	10.8 ± 0.4 ^c
G-CS/VCF15	22.7 ± 0.9 ^b	0.83 ± 0.09 ^b	14.7 ± 1.2 ^a
G-CS/VCF20	20.3 ± 1.2 ^{bc}	0.55 ± 0.14 ^e	12.2 ± 0.6 ^b
G-CS/VCF25	19.7 ± 1.9 ^{cd}	0.69 ± 0.12 ^{cd}	10.3 ± 0.4 ^{cd}

Values are given as mean ± standard deviation. Different superscript letters in the same column indicate significant differences ($p < 0.05$).

260°C, respectively. While the incorporation of leather fibers led to an increase of the temperatures, the incorporation of 20.0 wt% leather fiber in genipin crosslinked chitosan matrix increased the $T_{20\%}$ and T_{max} by 51°C and 9°C, respectively. The results suggest that the thermal stability of chitosan film was largely enhanced by the incorporation of VCF.

Mechanical properties

Results of the TS, YM and EAB for the chitosan-based films are shown in Table III. The TS of G-CS film was found to be 23.2 ± 1.0 MPa, which is comparable to that of the common synthetic plastic films such as high-density polyethylene (22-23 MPa) and low-density polyethylene (19-44 MPa).⁴⁴ The TS for the G-CS/VCF composite films with 5.0 wt% and 10.0 wt% VCF were 23.8 ± 1.1 and 25.5 ± 1.6 MPa, respectively. With an increase of VCF to 25.0 wt%, the TS decreased to 19.7 ± 1.9 MPa for G-CS/VCF25. Similar phenomenon has also been observed in nanocrystalline cellulose

(NCC)-reinforced chitosan films when the NCC is over 5%.⁴⁵ This is possibly due to the poor dispersion and entanglement of VCF induced by the addition of excess fiber. At the same time, Table III shows that the YM of the G-CS/VCF films was significantly lower than that of the G-CS film ($p < 0.05$). This is expected since the YM of the chitosan matrix is higher than that of the collagen fiber. The EAB for G-CS (control) was 8.6 ± 0.3%. The EAB values for G-CS/VCF composites were slightly but significantly higher than that of the control sample.

Dynamic mechanical analysis

Dynamic mechanical analysis (DMA) is a technique that has been extensively applied to characterize polymer materials. Analysis of the DMA data has given important information on the viscoelastic nature and transition state of the polymers. The DMA technique measures the stress-strain relationship of viscoelastic materials over a spectrum of temperature and time (or frequency). It is one

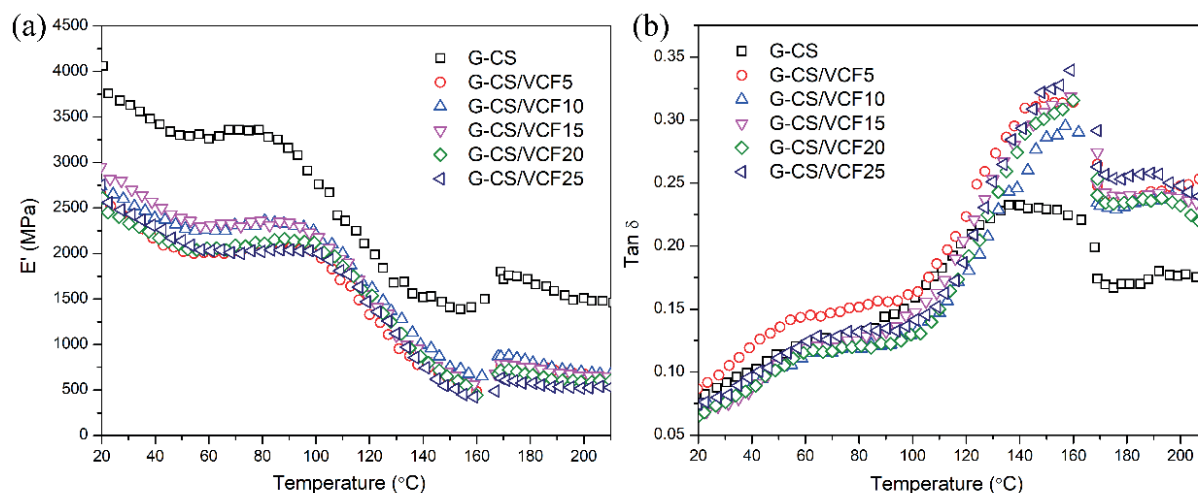


Figure 9. (a) Storage modulus (E') and (b) loss factor ($\text{Tan}\delta$) as a function of temperature for the genipin-crosslinked chitosan-based films.

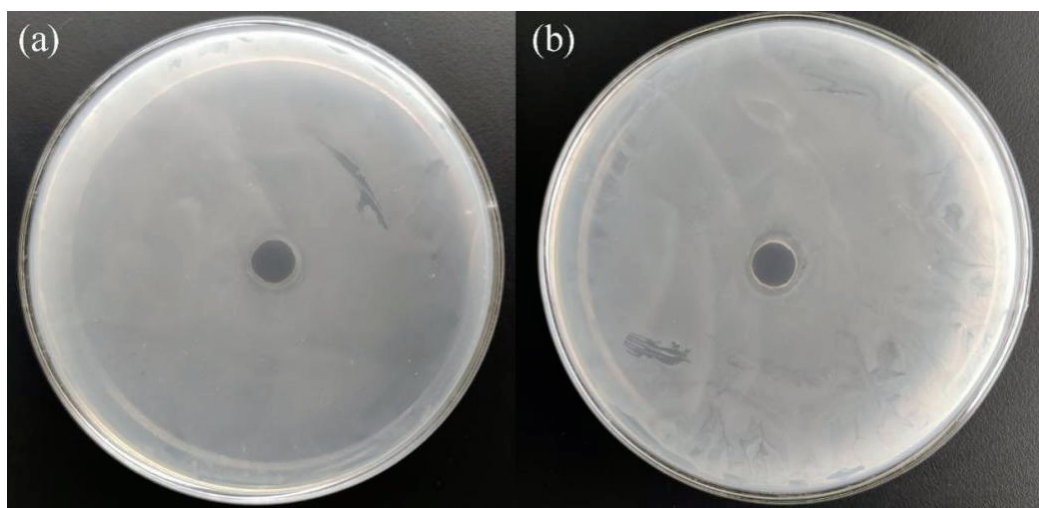


Figure 10. Preliminary agar diffusion test results of the genipin-crosslinked chitosan/VCF film (G-CS/VCF15) against (a) *E. coli* and (b) *S. aureus*.

of the most powerful tools for characterizing the molecular chain segment motion, intermolecular interactions, and interfacial interactions in polymer composites. Since composite materials can undergo various types and levels of dynamic stressing during fabrication and in service, studies on the viscoelastic behavior of these materials are of great importance. Figure 9 shows the dynamic storage modulus (E') and loss factor ($\text{Tan}\delta$) as a function of temperature for chitosan-based films containing different weight percentages of VCF.

The glass transition temperature (T_g) depends on the free volume of polymer. Below T_g , segmental movement of the main chain of the polymers is frozen, and the amount of free volume is smaller than the equilibrium. With an increase of temperature, the movement in the main chain happens at the T_g of the polymers, mainly the peak of $\text{Tan}\delta$, which is called α -relaxation. From Figure 9(a), it was found that the E' of all the G-CS/VCF films was lower than that of the G-CS film, even after the glass-rubber transition. The addition of 25.0 wt% of VCF yielded a 25% decrease of the storage modulus at 30 °C. The $\text{Tan}\delta$ -temperature ($\text{Tan}\delta$ -T) curves provide information about molecular damping. In Figure 9(b), the $\text{Tan}\delta$ -T curve of G-CS shows a broad peak centered around 150°C, and it exhibits a shift toward higher temperatures and a marked decrease in intensity with the addition of VCF. This peak was attributed to the glass transition of crosslinked chitosan. Similar T_g results were obtained

by Argin-Soysal et al. using a modulated DSC.⁴⁶ The $\text{Tan}\delta$ -T peak shift signifies the interaction between chitosan and leather fiber. Moreover, the $\text{Tan}\delta$ -T peak shift and intensity decrease may be related to the fact that VCF restricts the movement of the chitosan chains.

Preliminary evaluation of antibacterial activity

The antibacterial activity is an important factor for active packaging applications. Herein, both Gram-negative (*E. coli*) and Gram-positive (*S. aureus*) bacteria were used as experimental bacteria to assess the antibacterial properties of the composite films. Figure 10 shows the antibacterial activity of G-CS/VCF15, a representative sample, against these bacteria. After 24 h of incubation, inhibition zones appeared around the sample discs. These results clearly demonstrated that the G-CS/VCF composite films had preferable antibacterial activity against the above bacteria. The antibacterial activity of the film should be mainly ascribed to chitosan. The proposed antibacterial mechanisms of chitosan can be summarized as follows: cell membrane disruption; change in membrane permeability; leakage of intracellular constituents; and inhibition of microbe growth. Generally, chitosan has a more pronounced antibacterial effect against Gram-positive bacteria than Gram-negative bacteria due to the positive charge of chitosan.⁴⁷ This phenomenon was observed with clearer and larger inhibition zones for *S. aureus* than for *E. coli*.

Conclusions

In this study, composite films made from genipin-crosslinked chitosan and vegetable-tanned collagen fibers (VCF) were prepared using a solution casting method. FTIR and DMA results indicated that VCF was compatible with the chitosan substrate and formed additional hydrogen bonds. The analysis of SEM and XRD revealed that VCF was embedded in a continuous chitosan network. The properties of chitosan film were greatly affected by VCF incorporation. Compared with the control film without VCF, the composite films showed enhanced optical barrier performance, stability in water/aqueous medium, thermal stability and tensile strength. Furthermore, films containing VCF exhibited higher water vapor permeability, Young's modulus, and elongation at break than those of the control film. In addition, the composite film showed inhibitory effects against Gram-positive and Gram-negative bacteria, with potential application as packaging material. The results indicated that VCF can be used as a potential filling material to improve the practical value of chitosan films and provide a new approach for value-added utilization of solid leather waste.

Acknowledgments

The authors sincerely thank ARS, ERRC scientists: Joseph Uknalis for SEM photos, Jianwei Zhang for TGA and FTIR analysis, Lorelie Bumonlag for DSC analysis, Tony Jin for antibacterial tests, and Nicholas P. Latona for DMA tests and sample preparations. This work was supported by the Key Scientific Research Projects of Henan Province, China (grant number 21A430034).

References

1. Iwata, T.; Biodegradable and bio-based polymers: Future prospects of eco-friendly plastics. *Angewandte Chemie International Edition* **54**(11), 3210-3215, 2015.
2. Liu, J., Liu, C., Zheng, X., Chen, M. and Tang, K.; Soluble soybean polysaccharide/nano zinc oxide antimicrobial nanocomposite films reinforced with microfibrillated cellulose. *International Journal of Biological Macromolecules* **159**, 793-803, 2020.
3. Motelica, L., Fikai, D., Fikai, A., Oprea, O. C., Kaya, D. A., and Andronescu, E.; Biodegradable antimicrobial food packaging: Trends and Perspectives. *Foods* **9**, 1438, 2020.
4. Friedman, M. and Juneja, V. K.; Review of antimicrobial and antioxidative activities of chitosans in food. *Journal of Food Protection* **73**(9), 25, 2010.
5. Alishahi, A. and Aider, M.; Applications of chitosan in the seafood industry and aquaculture: A review. *Food and Bioprocess Technology* **5**(3), 817-830, 2012.
6. Adamiak, K. and Sionkowska, A.; Current methods of collagen cross-linking: Review. *International Journal of Biological Macromolecules* **161**, 550-560, 2020.
7. Sundar, V. J., Gnanamani, A., Muralidharan, C., Chandrababu, N. K. and Mandal, A. B.; Recovery and utilization of proteinous wastes of leather making: A review. *Reviews in Environmental Science and Bio/Technology* **10**(2), 151-163, 2011.
8. Wu, C., Zhang, W., Liao, X., Zeng, Y. and Shi, B.; Transposition of chrome tanning in leather making. *JALCA* **109**, 176-183, 2014.
9. Auad, P., Spier, F. and Gutterres, M.; Vegetable tannin composition and its association with the leather tanning effect. *Chemical Engineering Communications* **207**(5), 722-732, 2020.
10. Kolomaznik, K., Adamek, M., Anel, I. and Uhlirva, M; Leather waste - potential threat to human health, and a new technology of its treatment. *Journal of Hazardous Materials* **160**(2-3), 514-520, 2008.
11. Rigueto, C. V. T., Rosseto, M., Krein, D. D. C., Ostwald, B. E. P., Massuda, L. A., Zanella, B. B. and Dettmer, A.; Alternative uses for tannery wastes: A review of environmental, sustainability, and science. *Journal of Leather Science and Engineering* **2**(1), 21, 2020.
12. Liu, B., Li, Y., Wang, Q. and Bai, S.; Green fabrication of leather solid waste/thermoplastic polyurethanes composite: physically debundling effect of solid-state shear milling on collagen bundles. *Composites Science and Technology* **181**, 107674, 2019.
13. Liu, C.-K., Latona, N. P. and Taylor, M. M.; Preparations of nonwoven and green composites from collagen fibrous networks. *JALCA* **109**, 35-40, 2014.
14. Liu, J., Liu, C.-K. and Brown, E. M.; Development and characterization of genipin cross-linked gelatin based composites incorporated with vegetable-tanned collagen fiber (VCF). *JALCA* **112**, 410-419, 2017.
15. Xia, G., Sadanand V., Ashok, B., Reddy, K. O., Zhang, J. and Rajulu A. V.; Preparation and properties of cellulose/waste leather buff

- biocomposites. *International Journal of Polymer Analysis and Characterization* **20**(8), 693-703, 2015.
16. Teklay, A., Gebeyehu, G., Getachew, T., Yaynshet, T. and Sastry, T. P.; Preparation of value added composite boards using finished leather waste and plant fibers - a waste utilization effort in Ethiopia. *Clean Technologies and Environmental Policy* **19**(5), 1285-1296, 2017.
 17. Cavalcante, D. G. S. M., Gomes, A. S., Santos, R.J., Kerche-Silva, L. E., Danna, C. S., Yoshihara, E. and Job, A. E.; Composites produced from natural rubber and chrome-tanned leather wastes: Evaluation of their In vitro toxicological effects for application in footwear and textile industries. *Journal of Polymers and the Environment* **26**, 980-988, 2018.
 18. Muralidharan, V., Arokianathan, M. S., Balaraman, M. and Palanivel, S.; Tannery trimming waste based biodegradable bioplastic: Facile synthesis and characterization of properties. *Polymer Testing* **81**, 106250, 2020.
 19. Ambone, T., Joseph, S., Deenadayalan, E., Mishra, S., Jaisankar, S. and Saravanan, P.; Polylactic acid (PLA) biocomposites filled with waste leather buff (WLB). *Journal of Polymers and the Environment* **25**, 1099-1109, 2017.
 20. Liu, C., Huang, J., Zheng, X., Liu, S., Lu, K., Tang, K. and Liu, J.; Heat sealable soluble soybean polysaccharide/gelatin blend edible films for food packaging applications. *Food Packaging and Shelf Life* **24**, 100485, 2020.
 21. ASTM; Standard test methods for water vapour transmission of materials. Designation: E96-00. *Annual book of ASTM standards* 907-914, 2000.
 22. Yilmaz, O., Kantarli, I. C., Yuksel, M., Saglam, M. and Yanik, J.; Conversion of leather wastes to useful products. *Resources, Conservation and Recycling* **49**(4), 436-448, 2007.
 23. Zhang, L., Liu, J., Zheng, X., Zhang, A., Zhang, X. and Tang, K.; Pullulan dialdehyde crosslinked gelatin hydrogels with high strength for biomedical applications. *Carbohydrate Polymers* **216**, 45-53, 2019.
 24. Cui, L., Jia, J., Guo, Y., Liu, Y. and Zhu, P.; Preparation and characterization of IPN hydrogels composed of chitosan and gelatin cross-linked by genipin. *Carbohydrate Polymers* **99**, 31-38, 2014.
 25. Lawrie, G., Keen, I., Drew, B., Chandler-Temple, A., Rintoul, L., Fredericks, P. and Grøndahl, L.; Interactions between alginate and chitosan biopolymers characterized using FTIR and XPS. *Biomacromolecules* **8**(8), 2533-2541, 2007.
 26. Mi, F.-L., Shyu, S.-S. and Peng, C.-K.; Characterization of ring-opening polymerization of genipin and pH-dependent cross-linking reactions between chitosan and genipin. *Journal of Polymer Science Part A: Polymer Chemistry* **43**, 1985-2000, 2005.
 27. Kaczmarek, B., Sionkowska, A. and Stojkowska, J.; Characterization of scaffolds based on chitosan and collagen with glycosaminoglycans and sodium alginate addition. *Polymer Testing* **68**, 229-232, 2018.
 28. Falcão, L. and Araújo, M. E. M.; Tannins characterization in historic leathers by complementary analytical techniques ATR-FTIR, UV-Vis and chemical tests. *Journal of Cultural Heritage* **14**(6), 499-508, 2013.
 29. Rhim, J.-W., Hong, S.-In, Park, H.-M. and Ng, P. K. W.; Preparation and characterization of chitosan-based nanocomposite films with antimicrobial activity. *Journal of Agricultural and Food Chemistry* **54**(16), 5814-5822, 2006.
 30. Joseph, S., Ambone, T. S., Salvekar, A. V., Jaisankar, S. N., Saravanan, P. and Deenadayalan, E.; Processing and characterization of waste leather based polycaprolactone biocomposites. *Polymer Composites* **38**(12), 2889-2897, 2017.
 31. Ambrósio, J. D., Lucas, A. A., Otaguro, H. and Costa, L. C.; Preparation and characterization of poly (vinyl butyral)-leather fiber composites. *Polymer Composites* **32**(5), 776-785, 2011.
 32. Guo, J., Li, X., Mu, C., Zhang, H., Qin, P. and Li, D.; Freezing-thawing effects on the properties of dialdehyde carboxymethyl cellulose crosslinked gelatin-MMT composite films. *Food Hydrocolloids* **33**(2), 273-279, 2013.
 33. Butler, M. F., Ng, Y.-F. and Pudney, P. D. A.; Mechanism and kinetics of the crosslinking reaction between biopolymers containing primary amine groups and genipin. *Journal of Polymer Science Part A: Polymer Chemistry* **41**(24), 3941-3953, 2003.
 34. Paik, Y.-S. Lee, C.-M., Cho, M.-H. and Hahn, T.-R.; Physical stability of the blue pigments formed from geniposide of gardenia fruits: Effects of pH, temperature, and light. *Journal of Agricultural and Food Chemistry* **49**(1), 430-432, 2001.
 35. Liu, J., Zhang, L., Liu, C., Zheng, X. and Tang, K.; Tuning structure and properties of gelatin edible films through pullulan dialdehyde crosslinking. *LWT-Food Science and Technology* **138**, 110607, 2021.
 36. Ge, L., Xu, Y., Liang, W., Li, X., Li, D. and Mu, C.; Short-range and long-range cross-linking effects of polygenipin on gelatin-based composite materials. *Journal of Biomedical Materials Research Part A* **104A**, 2712-2722, 2016.
 37. Golub, D. and Krajnc, P.; Emulsion templated hydrophilic polymethacrylates. Morphological features, water and dye absorption. *Reactive and Functional Polymers* **149**, 104515, 2020.
 38. Liu, J., Liu, C., Zheng, X., Chen, M. and Tang, K.; Soluble soybean polysaccharide/nano zinc oxide antimicrobial nanocomposite films reinforced with microfibrillated cellulose. *International Journal of Biological Macromolecules* **159**, 793-803, 2020.
 39. Jin, J., Song, M. and Hourston, D. J.; Novel chitosan-based films cross-linked by genipin with improved physical properties. *Biomacromolecules* **5**, 162-168, 2004.
 40. Leceta, I., Guerrero, P. and de la Caba, K.; Functional properties of chitosan-based films. *Carbohydrate Polymers* **93**, 339-346, 2013.
 41. Liu, J., Luo, L., Hu, Y., Wang, F., Zheng, X. and Tang, K.; Kinetics and mechanism of thermal degradation of vegetable-tanned leather fiber. *Journal of Leather Science and Engineering* **1**, 9, 2019.
 42. Lavorgna, M., Piscitelli, F., Mangiacapra, P. and Buonocore, G. G.; Study of the combined effect of both clay and glycerol plasticizer on the properties of chitosan films. *Carbohydrate Polymers* **82**(2), 291-298, 2010.

43. Wang, S. F., Shen, L., Tong, Y. J., Chen, L., Phang, I. Y., Lim, P. Q. and Liu, T. X.; Biopolymer chitosan/montmorillonite nanocomposites: Preparation and characterization. *Polymer Degradation and Stability* **90**(1), 123-131, 2005.
 44. Hernandez, R. J., Selke, S. E. M. and Culter, J. D.; Major plastics in packaging, in *Plastics packaging: Properties, processing, applications, and regulations*. Hanser Gardner Publications, Inc.: Cincinnati, OH. 89-134, 2000.
 45. Khan, A., Khan, R. A., Salmieri, S., Le Tien, C., Riedl, B., Bouchard, J., Chauve, G., Tan, V., Kamal, M. R. and Lacroix, M.; Mechanical and barrier properties of nanocrystalline cellulose reinforced chitosan based nanocomposite films. *Carbohydrate Polymers* **90**(4), 1601-1608, 2012.
 46. Argin-Soysal, S., Kofinas, P. and Lo, Y. M.; Effect of complexation conditions on xanthan-chitosan polyelectrolyte complex gels. *Food Hydrocolloids* **23**(1), 202-209, 2009.
 47. Dutta, P. K., Tripathi, S., Mehrotra, G. K. and Dutta, J.; Perspectives for chitosan based antimicrobial films in food applications. *Food Chemistry* **114**(4), 1173-1182, 2009.
-

Avoiding the Production of Polluting and Toxic Chemicals in the Tanning Process

by

Josep M. Morera,^{1*} Esther Bartolí,¹ Patricia Rojas² and Luisa F. Cabeza¹

¹GREiA Research Group, Universitat de Lleida, Av. Pla de la Massa 8, 08700 Igualada, Spain.

²Accenture, Parque Empresarial Sant Joan, Plaça de Xavier Cugat, 2, 08174, Barcelona, Spain.

Abstract

Polluting and potentially toxic chemicals are used in tanning. Sodium sulfide/hydrosulfide are used when the hides are unhaired. These chemicals can be transformed into hydrogen sulfide with a simple change of pH. This gas is highly toxic and is the recurring cause of many deaths and accidents due to suffocation of workers in tanneries around the world. The basic salts of chromium III are the most used chemical to tan. The chromium III used can be transformed by oxidation, even once the leather transformed into a consumer good (shoes, for example), in chromium VI, which is carcinogenic. Both chemicals are present in process floats, in residual floats and in solid waste generated. Chromium III is also present in manufactured leathers. This article aims to describe the problems associated with the use of the aforementioned hazardous materials and deepen the possibility of using less toxic alternative processes to tan. The designed process allows to significantly reduce the pollutant load of the discharged wastewater, facilitates the reuse of the solid waste generated and clearly improve the safety of people at work.

Introduction

The tanning industry is considered very pollutant¹ due to the chemicals used. It is believed that the greatest risk of injuries connected with certain tasks is caused by the greater proximity or contact with agents potentially dangerous.² The tanning process follows different steps. Two of the most polluting steps are unhairing and tanning.³

The unhairing is part of the beamhouse processes, those that prepare the hide to be tanned. The traditional unhairing process is carried out to separate the hair from the hide with sodium sulfide and/or sodium hydrosulfide and lime.⁴ The combination of hydrosulfide (HS⁻) and hydroxyl (OH⁻) breaks the disulfide bonds of the keratin, main protein constituent of the hair, transforming the cysteine residues, not easily hydrolysable, in cystine residues, that dissolve easily in alkaline solutions. Equation (1) shows one of the possible mechanisms of this reaction:



It is a low-cost operation that poses little risks for the hide quality in the whole process. Nevertheless, although the efforts carried out by many researchers, it is still a very polluting process and with high health risk for the operators due to the use of sodium sulfide and sodium hydrosulfide as unhairing agent.

The pollution produced is high.⁵ Due to the organic matter detached when dissolving the hair and part of the hide, and to the used chemicals, the residual float has very high chemical organic demand (COD), suspended solids (SS), nitrogen (TKN), and toxicity (TOX). The worldwide total amount of water in beamhouse operations has been calculated⁶ in approximately 105 Mm³, which is about 60% the total amount of water used in all the tanning process.⁷ About 75% of COD, 80% of SS, 85% of TKN, and 100% of sulfide (S²⁻) are generated during beamhouse. Therefore, approximately 0.9 Mt of COD, 0.04 Mt SS, 0.08 Mt TKN and 0.6 Mt of S²⁻ are produced.

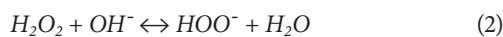
On the other hand, sulfide and hydrosulfide ions contained in both unhaired skins and residual floats from the unhairing operation are a major latent hazard. When, for any reason, the pH value of the float is less than 9, hydrogen sulfide is formed. This extremely toxic gas can cause great harm to the human body.⁸ Its inhalation has been the cause of numerous fatal accidents in the tanning industry.⁹ Inhalation of air with a concentration of 700 ppm of hydrogen sulfide causes instantaneous death. If the exposure is longer, the lethal concentration decreases. If the exposure lasts 30 minutes, a concentration of 500 ppm is already sufficient to produce unconsciousness and subsequent death.¹⁰ The danger of direct inhalation when opening the drum is not the only one. As the density of hydrogen sulfide is higher than that of air, it usually accumulates in low places, for example, the sewage pipes of the unhairing floats, where it can cause casualties when maintenance is performed. It is the typical case of a confined space fatality.¹¹ Often several consecutive accidents occur: a first person falls unconscious (then becomes a victim) and then all others who, without the necessary protective equipment, come to their rescue¹² are also affected.

Another undesirable effect of the use of sodium sulfide is that the presence of sulfide and hydrosulfide ions in wastewater floats complicates and makes treatment in treatment plants more expensive.¹³

*Corresponding author email: josepmaria.morera@udl.cat
Manuscript received March 22, 2021, accepted for publication May 16, 2021.

Another drawback of the type of unhairing method mentioned is that solid wastes, called fleshings, which contain sulfide and are difficult and expensive to recycle and/or reuse are also generated. Although attempts have been made to reuse them in different ways, often such wastes are brought to a landfill.¹⁴

Several alternative processes have been developed to minimize the pollution generated and to eliminate or reduce the use of sodium sulfide in the traditional unhairing process. An example of this is the unhairing process that allows hair recovery without dissolving it and subsequently allows its separation from the residual float via filtration.¹⁵⁻¹⁹ Another alternative are oxidative unhairing processes, based on the use of unhairing products such as hydrogen peroxide and the like.²⁰⁻²⁴ Hydrogen peroxide, at pH values close to 13, is capable of hydrolyzing the hair through an oxidative reaction. The oxidative attack of the S-S bond is due to the formation of peroxy anion from hydrogen peroxide (Equation (2)):



All hydrogen peroxide is consumed. Because the sodium sulfide/hydrosulfide is not used, the toxicity and the problem of the environmental management of waste floats and solid waste decreases greatly. The generation of hydrogen sulfide is avoided, which increases the safety of workers.

Recently, unhairing systems based on the use of enzymes have also been tested.²⁵⁻²⁸ Both oxidative and enzymatic unhairing systems can be combined with hair recovery to reduce the pollution generated. Unfortunately, at present, there is no commercial enzyme-based chemical that can completely replace sodium sulfide as a depilatory agent.

Tanning with chromium III salts is also a problematic operation from an environmental point of view.²⁹ Chromium III binds to the carboxylic groups of the side chains of collagen,³⁰ thus stabilizing this protein. The hide, which once the animal is dead is easily degradable,³¹ is transformed into leather, which is a material suitable for manufacturing large quantities of consumer goods (bags, shoes, etc.).

The chromium III contained in the residual float of the tanning operation must be treated correctly to avoid serious pollution problems.³²

Subsequently, in many cases, the resulting sludge is deposited in a landfill. In addition, significant amounts of chrome shavings, which are also deposited in a landfill, are generated.³³ The main health problem of chromium III is that, under certain conditions, it can be oxidized to chromium VI, which is carcinogenic.³⁴ The chromium incorporated in the leather can suffer this oxidation due to the effect of solar radiation at relatively high temperatures.

There are other tanning agents, such as those based on vegetable extracts, which are eco-friendlier.³⁵ The tannins of these tanning agents react with the hide, mainly through hydrogen bridge bonds.

The replacement of chromium III salts is not always possible, because they confer different properties to the leather than those of other known tanning agents.³⁶ As in the case of the unhairing with sodium sulfide and lime, tanning with chromium salts is favored by its low cost and the ease of handling. However, every day there is more demand for products made of chrome-free leather.³⁷

The aim of this paper is to increase the knowledge that allows to develop more ecological tanning processes, minimizing the pollutant load discharged and using less toxic and dangerous chemicals for health. To achieve this goal, the influence of three innovative types of unhairing in leathers tanned with three different vegetable extracts has been studied. An experimental design of the Latin square type has been followed to carry out the experimentation and the results have been assessed by performing the corresponding statistical analysis.

Achieving such aim will bring new knowledge such as the changes in the physical properties of the final leather produced and the pollution dumped during the oxidant unhairing process comparing if the unhairing process dissolved the hair or not. This comparison is then compared with results from a classical reductive unhairing process.

In most of published research papers about an oxidant unhairing process, hides are tanned with chromium salts. Therefore, another novelty of this paper is the study of the compatibility and the behavior of vegetable tanning agents with different chemical base (two condensed and one hydrolysable) with the proposed oxidizing unhairing agents. This knowledge will contribute to better understand the mechanism of the chemical reaction between the oxidant unhairing agent and the hide.

Experimental

Materials

The tests were carried out using 0.85 m in diameter and 0.4 m wide stainless steel drums with rotating rate and temperature control. The machinery and the chemicals used in the processes were those normally used in the leather industry.

The chemicals used specifically in unhairing and tanning operations were: sodium hydroxide (50% w/w), calcium hydroxide (95% w/w), sodium sulfide (60% w/w), hydrogen peroxide (50% w/w), unhairing auxiliary based on secondary amines (Ribersal PLE Base) and unhairing auxiliary based on enzymes (Riberzym MPX) both provided by Cromogenia Units S.A., formic acid (85% w/w), ammonium sulfate (99% w/w), bating agent based on enzymes (Oropon OR) provided by TFL, phenolic pretanning

Table I
Experimental design

<i>Experimental design: variables and levels</i>									
Variable	Level								
	-1	0		1					
Part of the hide	Belly	Shoulder		Butt					
Unhairing type	Reductive	Ox. Rec.		Oxidative					
Vegetable extract type	Mimosa	Quebracho		Chestnut					
<i>Experimental design: latin square</i>									
	Mimosa	Quebracho		Chestnut					
Belly	Ox. Rec.	Oxidative		Reductive					
Neck	Oxidative	Reductive		Ox. Rec.					
Butt	Reductive	Ox. Rec.		Oxidative					
<i>Selected experiments</i>									
Experiment	1	2	3	4	5	6	7	8	9
Part of the hide	-1	0	1	-1	1	0	0	-1	1
Unhairing type	0	1	-1	1	0	-1	0	-1	1
Vegetable extract type	-1	-1	-1	0	0	0	1	1	1

agent (Basyntan RS-3) provided by BASF, naphthalene sulfonic pretanning agent (Blancotan SN-20) provided by Silva SRL and vegetable extracts of mimosa (68% w/w tannin content) provided by Tanac S.A., quebracho (72% w/w tannin content) provided by Unitan Saica and chestnut (76% w/w tannin content) provided by Silvateam.

The experiments were carried out three times. Three salted bovine hides were used in order to perform the tests.

Preliminary operations

The three hides were soaked to rehydrate them, and to remove the salt and dirt they contained. Subsequently, the subcutaneous tissue was removed with the fleshing machine.

Experimental design

The hide is anisotropic. Three clearly differentiated parts can be distinguished in terms of their structural properties: the shoulder or neck (upper part), the butt (central part) and the bellies (outer parts). This fact was taken into consideration when choosing the experimental design.

On the one hand, the influence on the physical properties of the leather obtained of three types of unhairing and three types of tanning was studied. On the other hand, the toxicity generated by each of the unhairing tested was compared.

To carry out the experimentation, a Latin square design was followed with three variables and three levels for each variable. The first variable considered was the hide part. Its three levels were the shoulder, the butt and the belly. The second variable was the type of unhairing. Its three variables were a classic reductive unhairing (Reductive), an oxidative unhairing with hair recovery (Ox. Rec.) and an oxidative unhairing with hair destruction (Oxidative). The third variable was the type of vegetable extract used in tanning. The three levels corresponded to each of the three most used vegetable extracts worldwide: mimosa, quebracho and chestnut. Table I shows the coded variables and levels, the selected experimental design and the nine experiments carried out.

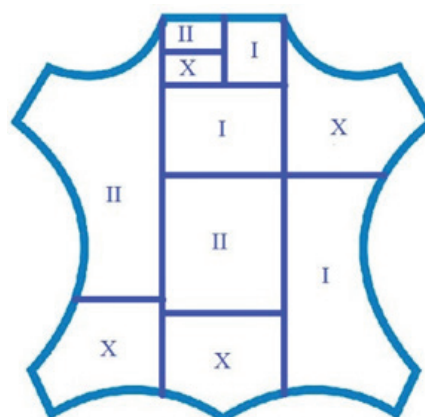


Figure 1. Sampling.

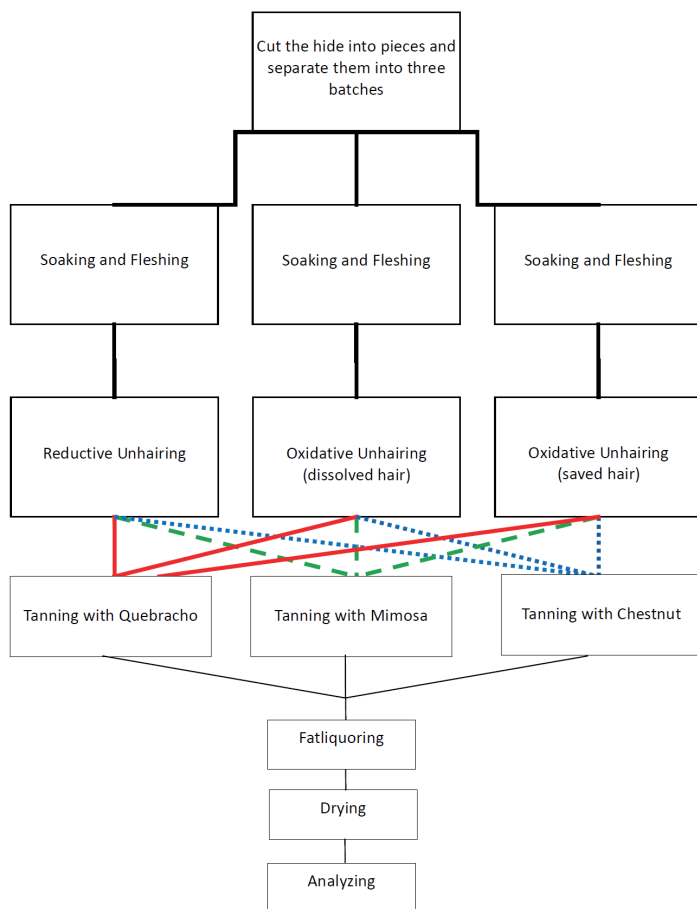


Figure 2. Procedure scheme.

Process

Each hide was cut into different pieces in order to carry out the nine tests (Figure 1).

Figure 2 shows an outline of the procedure followed to perform the nine tests.

The formulations used to perform the different tests are shown in Tables II and III. The formulation used for tanning (Table III) only varies in each case in the vegetable extract used.

Once tanned, the hides were fatliquored, dried and the following physical properties were analysed: tensile strength and elongation,³⁸ tear load,³⁹ distension and strength of grain,⁴⁰ and shrinkage temperature.⁴¹ With the results obtained, the statistical analysis was performed.

Samples of the residual floats from soaking to pickling were quantified and a representative sample of the mixture of the different floats was analyzed. The sulfide content (S²⁻) was determined through the Sulfide Test Kit, reference 114779, Merck brand, which is a photometric method. The “Toxicity” analyses were carried out according to the ISO 11348-3 norm. Analyses of Chemical Oxygen Demand (COD), Suspended Solids (SS), Conductivity and Nitrogen (TKN) were carried out according to the Standard Methods⁴².

Table II
Unhairing formulations

Reductive unhairing	Oxidative unhairing with dissolved hair	Oxidative unhairing with hair recovery
(% on fleshed weight):		
<i>Unhairing</i>	<i>Unhairing</i>	<i>Unhairing</i>
200% Water at 25°C	30% Water at 25°C	100% Water at 25°C
3% Sodium sulfide	0.2% Sodium hydroxide	0.5% Calcium hydroxide
4.5% Calcium hydroxide	Rotate 15 min. pH=10-11	Rotate 15 min. Drain
Rotate 8 hrs.	0.3% Amine product	200% Water at 25°C
Night at rest. pH = 12.8	Rotate 30 min	0.2% Sodium hydroxide
Drain and wash	6% Sodium hydroxide	1.5% Amine product
	4.5% Hydrogen peroxide	Rotate 15 min. pH=10-11
<i>Deliming and Bating</i>	Rotate until unhairing	0.1% Enzyme
100% Water at 37°C	pH =13	Rotate 1 hr
1.2% Ammonium sulfate	2% Formic acid	4.5% Sodium hydroxide
Rotate 30 min	200% Water	4.8% Hydrogen peroxide
0.5% Sodium bisulfite	Rotate 3 hrs. Night at rest	Rotate until unhairing
Rotate 15 min. pH=8	pH=8. Drain and wash	2% Formic acid
1% Bating agent		Rotate 3 hrs. Night at rest.
Rotate 45 min	<i>Bating</i>	pH=8. Hair filtration, drain and wash
Drain	150% Water at 30°C	
	0.6% Bating agent	<i>Bating</i>
	Rotate 45 min	150% Water at 30°C
	Drain	0.6% Bating agent
		Rotate 45 min
		Drain

Table III
Tanning with different vegetable extracts

Pickling

80% Water at 25°C

8% Sodium chloride

Rotate 20 min

1% Formic acid 1:5

0.5% Sulfuric acid 1:10

Rotate 2 hrs, night at rest. Drain pH=3.5

Tanning

80% Water at 25°C

6% Phenolic pretanning agent

3% Sodium chloride

Rotate 5 hrs. °Bé=7.5

1% Naphtalene sulfonic pretanning agent

30% Vegetable extract (Mimosa, Quebracho or Chestnut)

Rotate 8 hrs. pH=3.5-4

Results and Discussion

Table IV shows the results of the physical tests performed to the nine tests of the Latin square design.

An analysis of variance was carried out to determine which variables were significant and how they influenced the physical parameters obtained.

Table V indicates the analysis of variance performed for tear load. The P-value indicates whether a variable influences the result of a given parameter. The quantity $(1 - P\text{-value}) \times 100$ is the percentage of possibilities that the variable influences the result. In the case of leather, and taking into account the anisotropy of the raw material, it is considered that at P-value equal to or higher than 90%, such influence exists.

Once the relationship of the analyzed variable-parameter was established, this influence can be determined. The results of the P-value indicate that the variables “part of the hide” and “unhairing type” influences the tear load.

Figure 3 shows the “unhairing type” influence. In this case there are significant differences between all results. The unhaired hides with the oxidative unhairing with hair recovery show tear resistance values higher to those of the reductive unhairing and this in turn, presents them superior to those of the hides subjected to the oxidative unhairing with dissolved hair. The results obtained are related to the collagen denaturation capacity by each of the depilating agents tested and with the way they are applied.

The analysis of the variable “Part of the hide” shows that the values obtained in the bellies are slightly inferior to the rest.

Table IV
Physical tests results

Test	Tensile strength (N/mm ²)	Elongation (%)	Tear load (N/mm)	Grain strength (N)	Grain distension (mm)	Shrinkage temperature (°C)
1	28.14	31.6	148.1	88.1	11.78	78
2	24.08	31.6	106.4	124.2	11.43	77
3	33.40	29.6	134.1	169.7	10.37	77
4	18.27	42.2	87.6	66.0	12.58	82.5
5	35.67	35.6	157.4	173.6	11.66	79
6	31.58	50.2	132.8	111.6	13.41	83
7	35.26	47.8	150.5	114.7	10.95	69.5
8	32.54	52.7	120.8	141.2	12.15	70.5
9	15.31	46.5	96.8	94.5	10.90	71

Table V
Analysis of variance for Tear load (N/mm)

Source	Sum of Squares	Df	Mean Square	F-Ratio	P-Value
MAIN EFFECTS					
A: Part of the hide	235.049	2	117.524	9.13	0.0987
B: Unhairing type	4593.95	2	2296.97	178.51	0.0056
C: Vegetable extract type	70.1089	2	35.0544	2.72	0.2685
RESIDUAL	25.7356	2	12.8678		
TOTAL (CORRECTED)	4924.84	8			

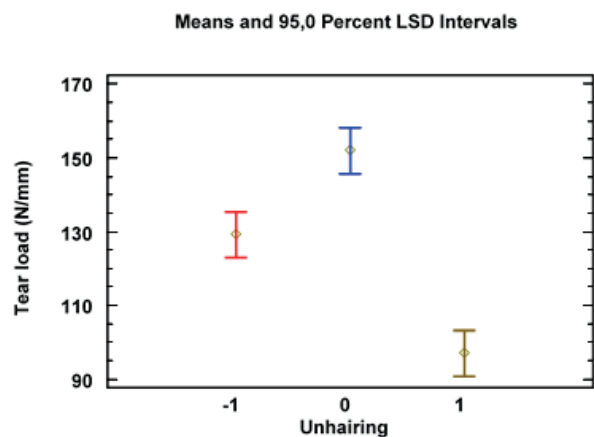


Figure 3. Influence of different unhairing systems on hide tensile strength (-1 = Reductive unhairing; 0 = Oxidative unhairing with saved hair; 1 = Oxidative unhairing with dissolved hair).

In the case of tensile strength, although clearly significant differences are not obtained, there is a trend that the lowest values are obtained with oxidative unhairing. This result would also be related to the collagen denaturation capacity by each of the depilating agents tested and with the way they are applied.

It is important to note in both cases that the values obtained in the leathers subjected to an oxidative unhairing with dissolved hair are clearly inferior to the rest. This result means that the oxidative unhairing with hair destruction hydrolyses more collagen fibers than the other two tested unhairing methods.

The analysis of the elongation results revealed that it depends only on the type of extract used (P -value = 0.0312). The tanned leathers with mimosa give significantly lower results than the others. The interpretation of these results is that the elongation depends on the type and number of bonds that are established between the collagen fibers and the vegetable extract used, which are mostly of the hydrogen bridge type. However, it should be remembered that the vegetable extracts used are not natural, they are chemically modified. This means that not all extracts from the same family behave the same.

Finally, it is found that the shrinkage temperature depends solely on the type of vegetable extract used as tanning agent (P = 0.0258). It is a logical result since the stabilization of collagen (degree of tanning) depends on the number and type of links between the collagen and the tanning agent. When quebracho or mimosa are used as tanning agent, higher shrinkage temperatures are obtained than chestnut is used.

The results of the physical tests make it possible to affirm that the leathers obtained by performing an oxidative unhairing and a tanning with vegetable extract are valid for manufacturing a

significant number of leather articles to be used, for example, in leather goods, upholstery or saddles.

It should also be highlighted that with the oxidative unhairing process with hair recovery, similar (or better) values of physical properties to those obtained with reductive unhairing are achieved; on the other hand, with the oxidative unhairing process with hair dissolution those values are lower. Taking into account that with the oxidative unhairing process with hair recovery more H_2O_2 and less NaOH are used than with the same unhairing process with dissolution of the hair, it could be considered that NaOH is responsible, directly or indirectly, for the greater hydrolysis of collagen fibers which results in the loss of resistance of the hide. Confirming this assumption would require specific research and would be interesting since it could open the door to solving one of the problems presented by the oxidative hairing removal studied, which is precisely the loss of physical resistance in the finished leather. This solution could come, for example, from the partial or total substitution of NaOH as a basifying agent.

Finally, it is shown that the type of chemical base of the commercial vegetable extract used only influences the shrinkage temperature. In the other physical properties analyzed, the results are independent of the type of vegetable extract used, which indirectly indicates that the behavior of the vegetable extracts is very similar, regardless of whether an oxidizing or reducing hairing process is used. This is in contrast to chrome salt tanning, where leathers subjected to oxidative unhairing absorb more chrome. This is surely due to the fact that due to oxidation, more carboxylic bonds appear in the hide. Chromium reacts with these bonds and tanning occurs. On the other hand, for tanning, the tannins of the vegetable extracts react preferentially via hydrogen bonding.

Figure 4 shows the results of the chemical analyses carried out to the residual floats.

Chemical analyses carried out to the residual floats revealed when a reductive unhairing is used, approximately 5 kg of HS^- per tonne of rawhide was wasted. This value is in accordance with that accepted by the International Union of Leather Technologists and Chemists Societies (IULTCS),⁶ which places this value between 2-9 kg of S^{2-} per tonne of rawhide. No sulfide was found in the analyses carried out in the residual floats of the two oxidative unhairing methods used. "Toxicity" results depended on the unhairing method: 1953 eq/t hide for the reductive unhairing, 190 eq/t hide for the oxidative unhairing with dissolved hair and 25 eq/t for the oxidative unhairing with hair recovery. As expected, replacing the unhairing product eliminates any presence of sulfide or hydrosulfide in the residual floats. Consequently, all toxicity problems related to hydrogen sulfide disappear. The use of hydrogen peroxide as an unhairing agent does not cause any toxicity problems, since at the end of the unhairing

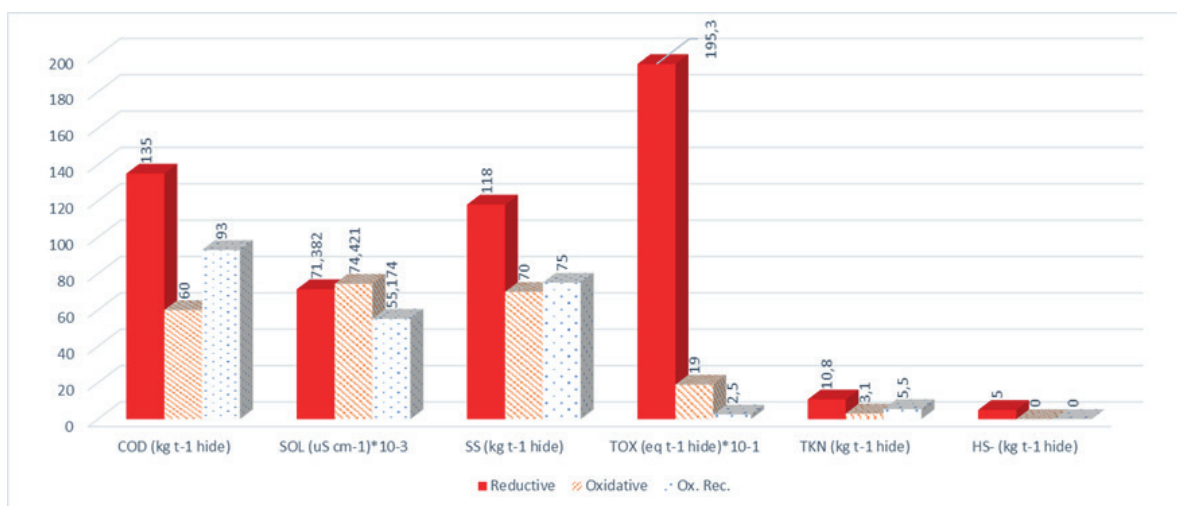


Figure 4. Pollution load of wastewater (Reductive = Reductive unhairing; Oxidative = Oxidative unhairing with dissolved hair; Ox. Rec. = Oxidative unhairing with hair recovery).

process the entire compound has been converted into water. The decrease in the main polluting parameters is also remarkable when replacing the Reductive unhairing with an Oxidative unhairing. In the case of Oxidative unhairing with dissolved hair, the COD decreased by 56%, the SS by 41% and the TKN by 71%. In the case of Oxidative unhairing with hair recovery, a 31% decrease in COD and SS and a 49% decrease in TKN was obtained.

Similarly, the substitution of chromium as tanning agent by the different vegetable extracts allowed to eliminate the presence of Cr III in the residual tanning floats, thus avoiding the risk of serious toxicological problems (mainly generation of Cr VI) that this product can produce.

Regarding the solid waste generated in the process, the absence of sulfides and chromium III greatly facilitates its reuse since it avoids having to carry out laborious and expensive processes to eliminate these toxic chemicals.

Conclusions

The results of the tests carried out show that many leather items suitable for various purposes (leather goods, upholstery, saddles, etc.) can be manufactured avoiding the latent toxicity problems involved in the use of hazardous materials such as sodium sulfide / hydrosulfide and chrome salts. These compounds, in themselves highly polluting, can be transformed into others (hydrogen sulfide and chromium VI) that are very harmful to human health, and can lead to the death of the person affected by inhalation or intake. The replacement of the reductive unhairing by an oxidative one and the replacement of the tanning chromium salts by vegetable extracts makes it possible to manufacture leathers bypassing the mentioned hazards, significantly reducing the pollutant load of wastewater and greatly facilitating the reuse of solid waste.

Acknowledgements

The authors of this paper would like to thank the Catalan Government for the quality accreditation given to their research group (2017 SGR 1537). GREiA is certified agent TECNIO in the category of technology developers from the Government of Catalonia. This work is partially supported by ICREA under the ICREA Academia programme.

References

- Heidemann, E.; Fundamentals of leather manufacturing, first ed. Eduard Roether KG, Darmstad, pp. 20, 1993.
- Ciarapica, F.E., Giacchetta, G.; Classification and prediction of occupational injury risk using soft computing techniques: An Italian study. *Saf. Sci.* **47**, 36-79, 2009. <https://doi.org/10.1016/j.ssci.2008.01.006>
- Tadesse, G.L., Tekalign, K.G.; Impacts of tannery effluent on environments and human health. *Environ. Earth Sci.* **7**, 88-97, 2017.
- Andrioli, E., Gutterres, M.; Associate use of enzymes and hydrogen peroxide for cow hides hair removal. *JALCA* **109**, 41-48, 2014.
- Tamersit, S., Bouhidel, K-E., Zakaria, Z.; Investigation of electro dialysis anti-fouling configuration for desalting and treating tannery unhairing wastewater: Feasibility of by-products recovery and water recycling. *J. Environ. Manag.* **207**, 334-340, 2018. <https://doi.org/10.1016/j.jenvman.2017.11.058>
- IULTCS, 2018. IUE- 6: Pollution values from tannery processes under conditions of good practice. International Union of Leather Technologists and Chemists (IULTCS) Database. http://www.iultcs.org/pdf/IUE_6.pdf (accessed January 2021).
- Buljan, J., Král', I.; The framework for sustainable leather manufacture, second ed., United Nations Development Organization, Vienna (Austria), pp. 31, 2018.

8. Xu, J-H., Fan, Y.; An individual risk assessment framework for high-pressure natural gas wells with hydrogen sulfide, applied to a case study in China. *Saf. Sci.* **68**, 14-23, 2014. <https://doi.org/10.1016/j.ssci.2014.02.013>
9. Yongsiri, C., Vollertsen, J., Hvitved-Jacobsen, T.; Effect of Temperature on Air-Water Transfer of Hydrogen Sulfide. *J. Environ. Eng.* **130**, 104-109, 2004. [https://doi.org/10.1016/\(ASCE\)0733-9372\(2004\)130:1\(104\)](https://doi.org/10.1016/(ASCE)0733-9372(2004)130:1(104))
10. OSHA; Web of United States Department of Labor. Occupational Safety and Health Administration (OSHA), 2020. <https://www.osha.gov/SLTC/hydrogensulfide/hazards.html> (accessed January 2021).
11. Selman, J., Spickett, J., Jansz, J., Mullins, B.; An investigation into the rate and mechanism of incident of work-related confined space fatalities. *Saf. Sci.* **109**, 333-343, 2018. <https://doi.org/10.1016/j.ssci.2018.06.014>
12. Barbera, N., Montana, A., Indorato, F., Arbouche, N., Romano, G.; Domino effect: An unusual case of six fatal hydrogen sulfide poisonings in quick succession. *Forensic Sci. Int.* **260**, e7-e10, 2016. <https://doi.org/10.1016/j.forsciint.2016.01.021>
13. Dixit, S., Yadav, A., Dwivedi, P.D., Das, M.; Toxic hazards of leather industry and technologies to combat threat: a review. *J. Clean. Prod.* **87**, 39-49, 2015. <https://doi.org/10.1016/j.jclepro.2014.10.017>
14. Ramesh, R.R., Muralidharan, V., Palanivel, S.; Preparation and application of unhairing enzyme using solid wastes from the leather industry—an attempt toward internalization of solid wastes within the leather industry. *Environ. Sci. Pollut. R.* **25**, 2121-2136, 2018. <https://doi.org/10.1007/s11356-017-0550-9>
15. Frendrup, W.; United Nations Industrial Development Organization Database. 2000. http://www.unido.org/fileadmin/user_media/Publications/Pub_free/Hair_save_unhairing_methods_in_leather_processing.pdf (accessed January 2021).
16. Valeika, V., Baleska, K., Valeikiene, V., Kolodzeiskis, V.; An approach to cleaner production: from hair burning to hair saving using a lime-free unhairing system. *J. Clean. Prod.* **17**, 214-221, 2009. <https://doi.org/10.1016/j.jclepro.2008.04.010>
17. Galarza, B.C., Cabello, I., Greco, C.A., Hours, R., Schuldt, M.M., Cantera, C.S.; Alternative technologies for adding value to bovine hair waste. *J. Soc. Leather Tech. Ch.* **94**, 26-32, 2010.
18. Lili, K., Jinwei, Z., Wuyong, C.; Composition, structure and properties of immunized hair from hair-saving unhairing process. *J. Soc. Leather Tech. Ch.* **99**, 124-128, 2015.
19. Valeika, V., Širvaitytė, J., Bridžiuvienė, D., Švedienė, D.; An application of advanced hair-save processes in leather industry as the reason of formation of keratinous waste: few peculiarities of its utilization. *Environ. Sci. Pollut. R.* **26**, 6223-6233, 2019. <https://doi.org/10.1007/s11356-019-04142-0>
20. Marmer, W.N., Dudley, R.L., Gehring, A.G.; Rapid oxidative unhairing with alkaline peroxide. *JALCA* **98**, 351-358, 2003.
21. Anzani, C., Prandi, B., Buhler, S., Tedeschi, T., Baldinelli, C., Sorlini, G., Dossena, A., Sforza, S.; Towards environmentally friendly skin unhairing process: A comparison between enzymatic and oxidative methods and analysis of the protein fraction of the related wastewaters. *J. Clean. Prod.* **164**, 1446-1454, 2017. <https://doi.org/10.1016/j.jclepro.2017.07.071>
22. Kanagaraj, J., Panda, R.C., Senthilvelan, T.; Green remediation of sulfide in oxidative dehairing of skin and correlation by mathematical model: An eco-friendly approach. *Process. Saf. Environ. Protect.* **100**, 36-48, 2016. <https://doi.org/10.1016/j.psep.2015.12.005>
23. Morera, J.M., Bartolí, E., Gavilanes, R.M.; Hide unhairing: achieving lower pollution loads, decreased wastewater toxicity and solid waste reduction. *J. Clean. Prod.* **112**, 3040-3047, 2016. <https://doi.org/10.1016/j.jclepro.2015.11.028>
24. Puccini, M., Seggiani, M., Castiello, D., Vitolo, S.; DEPOXO process: Technical and environmental study of hide oxidative unhairing. *Chem. Eng. Trans.* **36**, 193-198, 2014. <https://doi.org/10.3303/CET1436033>
25. Catalán, E., Komilis, D., Sánchez, A.; A Life cycle assessment on the dehairing of rawhides: chemical treatment versus enzymatic recovery through solid state fermentation. *J. Ind. Ecol.* **23**, 361-373, 2019. <https://doi.org/10.1111/jiec.12753>
26. Ranjithkumar, A., Durga, J., Ramesh, R., Sundar, V. J., Rose, C., Muralidharan, C.; Studies on alkaline protease from bacillus crolab MTCC5468 for applications in leather making. *JALCA* **112**, 232-239, 2017.
27. Chen, M., Jiang, M., Chen, M., Cheng, H., 2018. Approach towards safe and efficient enzymatic unhairing of bovine hides. *JALCA* **113**, 59-64, 2018.
28. Tian, J., Long, X., Tian, Y., Shi, B.; Eco-friendly enzymatic dehairing of goatskins utilizing a metalloprotease high-effectively expressed by *Bacillus subtilis* SCK6. *J. Clean. Prod.* **212**, 647-654, 2019. <https://doi.org/10.1016/j.jclepro.2018.12.084>
29. de Aquim, P.M., Hausen, E., Gutterres, M.; Water reuse: An alternative to minimize the environmental impact on the leather industry. *J. Environ. Manag.* **230**, 456-463, 2019. <https://doi.org/10.1016/j.jenvman.2018.09.077>
30. Oruko, R.O., Selvarajan, R., Ogola, H.J.O., Edokpayi, J.N., Odiyo, J.O.; Contemporary and future direction of chromium tanning and management in sub Saharan Africa tanneries. *Process. Saf. Environ. Protect.* **133**, 369-386, 2020. <https://doi.org/10.1016/j.psep.2019.11.013>
31. Covington, A.; Tanning chemistry: The science of leather., first ed. RSC Publishing, Cambridge, pp. 195, 2011.
32. Mella, B., Glanert, A.C., Gutterres, M.; Removal of chromium from tanning wastewater and its reuse. *Process. Saf. Environ. Protect.* **95**, 195-201, 2015. <https://doi.org/10.1016/j.psep.2015.03.007>
33. Cao, S., Liu, B., Cheng, B., Lu, F., Wang, Y., Li, Y.; Mechanisms of Zn (II) binds to collagen and its effect on the capacity of eco-friendly Zn-Cr combination tanning system. *J. Hazard. Mater.* **321**, 203-209 2017. <https://doi.org/10.1016/j.jhazmat.2016.09.016>

34. Jing, C., Nan, Z., Wuyong, C., Shiyu, S.; Controlling Cr VI in leather: A review from passive prevention to stabilization of chromium complexes. *JALCA* **112**, 250-257, 2017.
 35. Griyanitasari, G., Pahlawan, I.F., Kasmudjiastuti, E.; IOP Conf. Series: *Materials Science and Engineering* **432**, 012040, 2018. <https://doi.org/10.1088/1757-899X/432/1/012040>
 36. Jia, L., Ma, J., Gao, D., Tait, W.R.T., Sun, L.; A star-shaped POSS-containing polymer for cleaner leather processing. *J. Hazard. Mater.* **361**, 305-311, 2019. <https://doi.org/10.1016/j.jhazmat.2018.08.093>
 37. Krishnamoorthy, G., Sadulla, S., Sehgal, P.K., Mandal, A.B.; Green chemistry approaches to leather tanning process for making chrome-free leather by unnatural amino acids. *J. Hazard. Mater.* **215-216**, 173-182, 2012. <https://doi.org/10.1016/j.jhazmat.2012.02.046>
 38. ISO 3376:2020 [IULTCS/IUP 6]; Leather — Physical and mechanical tests — Determination of tensile strength and percentage elongation, 2020. <https://www.iso.org/standard/75173.html> (accessed January 2021).
 39. ISO 3377-2:2016 [IULTCS/IUP 8]; Leather — Physical and mechanical tests — Determination of tear load — Part 2: Double edge tear, 2016. <https://www.iso.org/standard/68861.html> (accessed January 2021).
 40. ISO 3379:2015 [IULTCS/IUP 9]; Leather — Determination of distension and strength of surface (Ball burst method), 2015. <https://www.iso.org/standard/63871.html> (accessed January 2021).
 41. ISO 3380:2015 [IULTCS/IUP 16]; Leather — Physical and mechanical tests — Determination of shrinkage temperature up to 100 °C, 2015. <https://www.iso.org/standard/61792.html> (accessed January 2021).
 42. APHA; Standard Methods for the Examination of Water and Wastewater, 20th ed. American Public Health Association, Washington, DC, 1998.
-

Role of Anionic Chromium Species in Leather Tanning

by

Abhinandan Kumar^a, Jaya Prakash Alla^a, Deepika Arathanaikotti^b, Ashok Raj J^b, Chandrababu N K^b

^aRegional Centre for Extension & Development (RCED) Kanpur, ^bLeather Process Technology Department, Central Leather Research Institute (CLRI), Council of Scientific and Industrial Research (CSIR), Adyar, Chennai-600020, India

Abstract

Chrome tanned leathers are definitely unique in comparison with leather made from any other known tanning agents, especially in terms of thermal stability, cost and its reactive mechanism with collagen fibers. In our current studies, self basifying chrome tanning materials masked with different percentages of organic acid were prepared and applied after the de-liming stage of leather processing. This eliminated the need for pickling and basification steps. Tanned leathers resisted shrinkage up to 103 and 105±2°C while conventional chrome tanned leathers resisted up to 108±2°C. Also, interaction of anionic chrome species in tanning was studied. It was observed that the percentage of anionic species in the experimental chrome tanning material was higher than conventional chrome tanning material and the shrinkage temperature achieved by application of experimental tanning material proves that anionic species do involve in tanning. Tanned leathers were crusted and analysed for strength and organoleptic properties.

Introduction

Tanning is one of the important stages in leather processing for conversion of raw hides/ skins into leather. Tanning was practiced since ancient times and primary tanning material used were plant polyphenols of different origins,¹ these tanned leathers were used for broad array of applications ranging from clothing, footwear, strapping materials, etc.

Modern inventions lead to development of chrome tanning material in the 19th century, which revolutionised the tanning industry. Chrome tanning was initially done in two bath system² where acidified chromic (VI) oxide was treated with skins or hides and then reduced using a reducing agent in another bath. Various other methods for preparing tanning materials^{3,4} were developed over the course of time. Single bath systems, self-basifying chrome liquors etc., were popular but the most widely accepted chrome tanning material is basic chromium sulphate (BCS). Numerous procedures have been reported for making chrome tanning material but the difference in properties vary with the type of acid and reducing agents employed; most common reducing agents being molasses, glucose and sugar.⁵ BCS tanning material is popular because of its ease in tanning, high thermal stability and low cost. Currently, chrome tanned leathers account for majority share of about 70-90% of total leathers produced.⁶

Conventional chrome tanning system utilizes up to 70% of the tanning material, thus lower exhaustion rates of tanning material contribute to higher chromium oxide content to discharge in effluent making chrome tanning effluent unfriendly to environment. Self basifying chrome tanning agents which automatically can adjust the final tanning bath pH are viable options and this type of system can increase the uptake capability of chrome tanning material by up to 95-98%.⁷

Basic chromium sulphate (33% basicity) is prepared by the reduction of hexavalent chromium with organic or inorganic reducing agents and contains up to 24-25% chromium as Cr₂O₃. Although the half-life of chromium species is in the range of several hours because of their kinetic inertness; many complex species persist for relatively longer periods of time in solution.⁸ More than fifteen species of chromium are present in a typical chrome tanning salt, varying in the degree of polymerisation, charge present on the complex, nature and number of ligands attached to central chromium atom. These species are found to be in equilibrium when in aqueous solution. The unspent chrome liquor contains 50-60% of +3 and +4 charged species,⁹ increase in the percentage of +3 charged species in spent chrome liquor (43%) from the freshly prepared chrome liquor (13-14%) shows that the species with charge other than +3 may have better affinity for protein and the conversion of other species to +3 charged species may be taking place during tanning.¹⁰

Chromium species differ in their kinetic lability and thermodynamic affinity towards the reactive sites of collagen.¹¹ Some species are kinetically so inert that they do not bind to collagen within the stipulated time for tanning and as a result one third of the total BCS used during tanning remains in effluent.¹² Chromium concentration in terms of total chromium in exhaust chrome liquor ranges from 1500-5000 mg/L.¹³

In this study anionic chromium complex with suitable ligands have been prepared and were used for tanning of skins. Anionic species were extracted and analysed using column chromatography. Leathers thus produced have been tested for shrinkage temperature, color measurement and physical strength properties. Experimental chrome tanned leathers found to be at par with the conventional chrome tanned leathers. Final tanning effluent liquor was also analysed for exhaustion of the chrome tanning material, Chemical Oxygen Demand (COD), and Total Solids (TS).

*Corresponding author email: sclriak1@gmail.com

Manuscript received April 6, 2021, accepted for publication May 19, 2021.

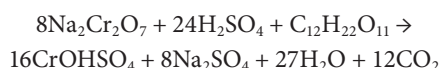
Experimental Section

Reagents

Basic chromium sulphate from Vishnu Chemicals Pvt. Ltd. India. Oxalic acid, sodium dichromate and sulphuric acid procured from SD Fine Chemicals India Pvt. Ltd. Alkaline bate from Tex Bio sciences India Pvt. Ltd. Sodium chloride, formic acid and sulphuric acid acquired from Rankem India Pvt. Ltd. Ammonium chloride, sodium formate and sodium bicarbonate were purchased from Merk Chemicals India Pvt. Ltd. Dowex resin (1X4 chloride form) was purchased from Sigma Aldrich.

Preparation of tanning material

Basic chromium sulphate (33% basicity) was prepared from the stoichiometric amount of sodium dichromate using glucose as reducing agent.¹⁴ The reaction may process as below



Bi- dentate ligands such as oxalic acid were used for complexation in the molar ratio 1:0.45 (B45) and 1:0.6 (B60) to the chrome liquor at 70°C with constant stirring. Final product was cooled to room temperature. The final pH adjusted to 3.0 using sodium carbonate. Prepared tanning material was analysed for Cr₂O₃ content.¹⁵

Anion Exchange chromatography

Ion exchange chromatography was performed for the 10% aqueous solution of chromium complexes prepared and were passed through a column of 30 cm length and 1 cm diameter using Dowex Resin (1X4 chloride form). Anionic chromium species held by the stationery phase were eluted first with 1N NaCl and then with 2N NaCl solution. Anionic species present in the chromium solutions were estimated.

A control was run with commercial BCS powder with the same process and ion exchange chromatography was done for 10% solution with the same.

Particle size

Hydrodynamic diameters of chrome tanning agent in solution were determined using Dynamic light scattering (DLS) with high performance particle analyser (Zetasizer Nano series, Malvern) at 25°C. This instrument operates at 4 mW He-Ne laser power, scattering angle of 173° and wavelength of 633 nm.

Application as tanning material

Application of prepared tanning material was checked at tanning stage of leather processing. Detail description was mentioned in Table I. The chromium complexes were applied on de-limed goat skins. Chromium solution of 8% on pelt weight basis was offered in

Table I

Process employed for control and experimental chrome application

Process: Wet Blue Leather

Raw Material: De-limed Goat Skins

Percentage of chemicals added on limed skin weight basis

Markings: Process: Control (C)- BCS (Conventional), Experiment (E)- B45, B60

Process Description	Chemicals	Percentage (%)		Time in Minutes	Remarks
		C	E*		
					*Similar procedure followed for application of B45 and B60 tanning materials
Washing					
	Water	200	200	10	Wash/Drain
Pickling					
	Water	80	-		
	Sodium chloride	8	-	10	
	Formic acid	0.5	-	15	
	Sulphuric acid	0.3	-	In 3 feeds at 15 interval + 30 run	In 1: 10 dilution with water
					Adjust pH to 3
Tanning					
	Water		50		
	Pickle Bath	40	-		From previous stage of processing
	Chrome Tanning agent	4	4	30	
	Chrome Tanning agent	4	4	60	
	Water	60	50	30	
Basification					
	Sodium Formate	0.5	-	15	
	Sodium Bi Carbonate	1.5	-	In 3 feeds at 15 interval + 30 run	In 1: 10 dilution with water
					Adjust pH to 4-4.2

two feeds; initial offer 4% with 50% water and drum was rotated for 30 min at 4-6 rpm. Second feed was offered and drum was rotated for another 1 hr for uniform distribution of chromium and further 50% of water was added. Finally, the drum was rotated for another 30 min to attain uniform pH of 4-4.2. Leathers were rinsed and piled. Control leathers were made from pickled skins, tanning was done with 50% pickle float with 4% BCS tanning material on pelt weight basis was added to drum and rotated of 45 min and another 4% was added and rotated for another 45 min, additional 50% water added and finally leathers were basified using 0.5% sodium formate and 1.5% sodium bicarbonate in 1:10 dilution with water in three instalments of 10 min each. Final pH was set to 4 and drum was rotated for another 30 min and leathers were rinsed and piled on horse (wooden stand for piling leathers). Spent chrome liquor from experiment (B45 and B60) and control (BCS) were analysed for chromium exhaustion. Description of the leather processing is mentioned in Table I.

Exhaustion Studies and wastewater analysis

Exhaustion studies were done by estimation of total Cr_2O_3 content present in the final tanning solution after completion of tanning process.¹⁵ Chemical Oxygen Demand (COD)¹⁶ and Total Solids (TS)¹⁷ in the effluent were also analysed. Water auditing from pickling to basification stages were also undertaken.

Scanning electron microscopy (SEM) analysis

SEM micrographs of crust leathers were studied using VEGA 3 SBU (TESCAN Orsay Holding) scanning electron microscope operating at 200V to 30kV at room temperature of 25°C and relative humidity of 50%. Leather samples were sputter coated with a thin layer of gold prior to examination. Samples were cut into 5x2cm² sections and mounted on adhesive stub for examination; samples were viewed for studying surface as well as cross section of the leather.

Physical strength properties and organoleptic properties

The samples for physical testing were cut from control and experimental glove leathers. The samples were conditioned to the required relative humidity of 65±2% at 20±2°C for 48 h.¹⁸ The tensile strength was measured as per the standard procedures¹⁹ and compared with UNIDO norms.²⁰ Values reported were average of four samples.

Organoleptic properties such as softness, fullness, grain smoothness and general appearance were evaluated by experienced leather technologists using a rating scale of 0-10 points for each functional property, where higher points indicate better properties exhibited.

Table II
Ion exchange chromatography of chrome species

	Cationic and non-ionic species (%)	Anionic -1 specie (%)	Anionic -2 specie (%)
Control	90	-	-
B45	35.65	58.86	5.48
B60	46.61	49.58	3.8

Results and Discussion

Speciation of chrome liquor prepared

Dicarboxylic acids are well known masking agents, reaction of dicarboxylates with single metal ion produce cyclic, chelate complexes with reduced activity. When the dicarboxylates form cross linkages between two metal ions the molecular size increases and so does its reactivity.⁸ Oxalates are bidentate ligands which can either act as a bridge between two metal centers or can form a chelate. By increasing the molar ratio of oxalic acid, it forms more bridges between metal centers than getting attached with single metal ion and therefore the positive charge on a metal complex is neutralized to a lesser extent resulting in the formation of less anionic species and masking of labile sites occurs. From Table II, ion exchange chromatography shows that there was a reduction in the percentage of both -1 and -2 chromium species as the molar ratio of oxalic acid was increased from 0.45 to 0.6. High exhaustion of 93 and 94% for B45 and B60 tanning material was observed with anionic species to an extent of 64.34% and 53.38%, respectively in the tanning solution. This indicates that anionic species are also participating in chrome tanning process of hides and skins. Commercial BCS containing higher percentage of positive charged species do not penetrate in the skin matrix at the higher pH as it gets fixed with the ionized carboxylic groups of collagen side chains making the penetration difficult. In case of anionic species, the interaction between the charged carboxylic groups and the chromium complex was restricted at the initial stages and later upon hydrolysis, fixation takes place.

Analysis of tanning material

Tanning materials B45 and B60 contained chrome content of 16.8% with basicity²¹ of 27%, while commercial BCS had 25% of Cr_2O_3 with basicity around 32-35%. Particle size of the B45 and B60 tanning material were in the range of 585 and 550±50nm while control BCS was measured to be around 300±10nm. Bigger particle size of experimental tanning material was due to anionic ligands acting as linkage between chromium complexes to form poly nuclear complexes.²²

Table III
Comparison of wet blue leathers

	Shrinkage Temperature (°C)	Exhaustion (%)	Final pH
Control	108±2	68±2	4
B45	103±2	93±3	4.2
B60	105±2	95±3	4.5

Leather application

Prepared chrome tanning materials B45, B60 and control as BCS were applied at the tanning stage of leather processing. Experimental chrome tanning materials were applied after de-liming. Uptakes of tanning materials were found to be higher in case of experimental leathers and exhaustion levels were 93 and 95% in case of B45 and B60 tanning materials. Final leathers were aged for 48 hours after tanning and were analysed for shrinkage temperature. From Table III, shrinkage temperature of experimental chrome tanned leathers have resisted temperature in par with conventional BCS tanned leathers.

Scanning electron microscopy analysis

Scanning electron microscopy images showing the grain surface of commercial and experimental chrome tanned leathers at magnification of 150× and cross section of at magnification of 500× can be seen from Figure 1. Grain surface of the leathers was uniform. In case of B45, surface pores were slightly shrunk that might be due to the tanning at high alkaline pH, B60 tanned leather showed no shrinkage. Overall physical appearances of leathers were satisfactory. Fiber bundles were compact in case of B45 and B60 which indicates that the leathers produced were full and compact in nature. No looseness could be observed, increased fullness and tightness of the experimental leathers due to compactness of the fiber bundles, conventional BCS tanned leathers showed more spacing between fibers making leather empty.

Exhaustion and wastewater analysis

Effluent from the chrome tanning stage was analysed for COD, total solids and chromium was estimated as Cr_2O_3 and results were presented in Table IV. It can be observed that chrome content in effluent was reduced by 88 and 89% and there was a reduction in COD up to 35 and 50% when B45 and B60 high exhaust chromes

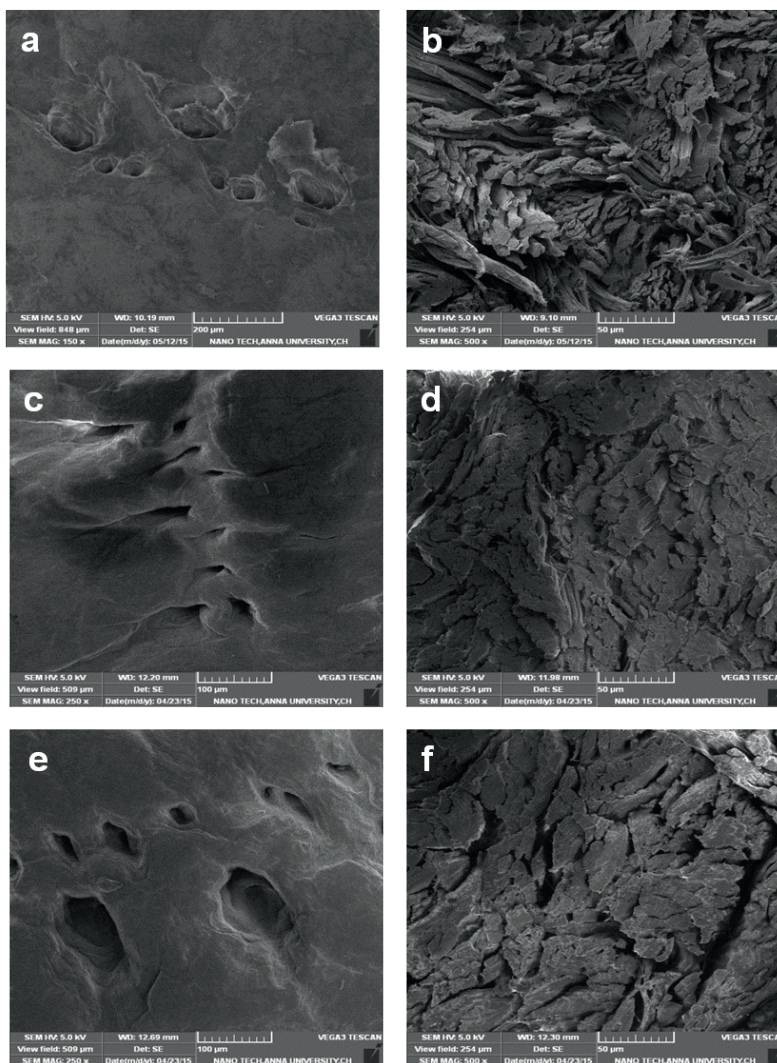


Figure 1. Scanning Electron Micrographs of chrome tanned leathers showing grain surface of a) control BCS, c) B45, e) B60 with magnification of 150× and cross section of b) control BCS d) B45 f) B60 with magnification of 500×

were used, also total solid content was reduced by 37 and 31% than conventional BCS processed effluent. Experimental leathers were processed at higher pH, where anionic chrome complexes were offered to the pelts. At such high pH most of the side chain carboxylic groups in collagen are found to be in ionized form which results in higher uptake of chromium and reduced chrome in the effluent.¹¹ The unit operations like Pickling and Basification have been completely eliminated during the experimental process. Thus, there was no offer of strong mineral acids or neutral salts which helps in significant reduction in TS and COD.

Water consumption in experimental tanning process was less, as pickling stage was completely avoided and there was a reduction of 44% in water consumption than control tanning process. Water audit was performed for pickling and tanning stage of leather processing, it was found that the conventional leather processing utilises up to 1.8L of water for processing one kilogram of hides/skins, while experimental chrome tanning with B45 and B60 tanning materials needed only 1L for processing one kilogram of hides/skins. There was a reduction of 44% with adoption of this pickle less and basification free system.

Table IV
Pollution load data from chrome tanning

	COD (mg/L)	Total Solids (mg/L)	Cr ₂ O ₃ in tanning effluent (mg/L)	COD reduction (%)	Reduction in Total Solids (%)	Reduction in Cr ₂ O ₃ (%)
Control	1600±20	26600±200	3300	-	-	-
B45	1040±20	16700±200	410	35	37	88
B60	800±20	18200±200	364	50	31	89

Table V
Comparison of mechanical properties of chrome tanned Upper Leather

	Tensile Strength (N/mm ²)	Elongation at break (%)	Grain Crack	
			Load(N)	Distance(mm)
Control	16±1	42±2	35±1	8±0.5
B45	15±0.5	51±2	30±1	11±0.5
B60	15±0.5	55±2	30±1	11±0.5
UNIDO standards	15	Not less than 40	-	-

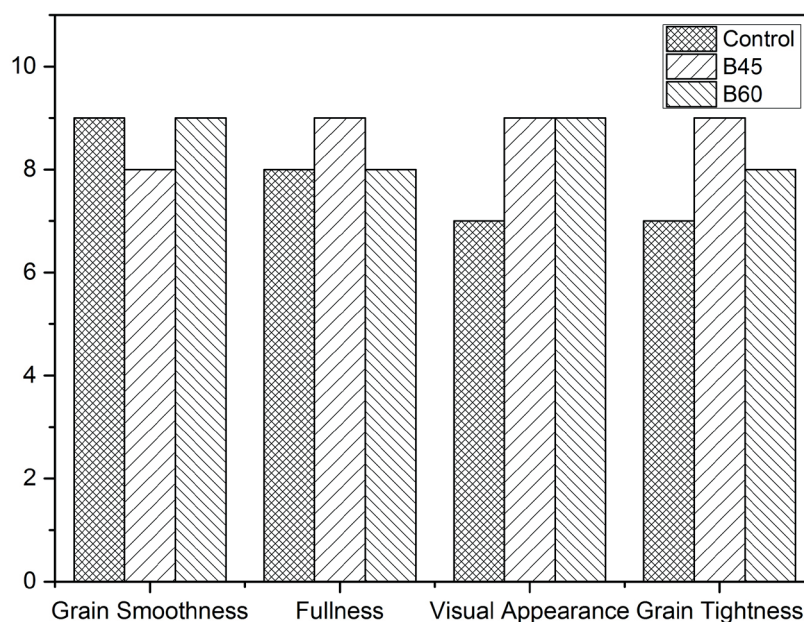


Figure 2. Comparison of organoleptic properties of upper leathers

Strength and organoleptic properties

Strength properties of the leathers tanned with experimental chrome tanning materials B45 and B60 were found to be in par with control BCS tanning material. All the leathers complied with UNIDO norms. From Table V, elongation at break values of B45 and B60 leathers elongated 21 and 30% higher, respectively than the conventionally tanned leathers, meaning increase in stretch ability of experimental leathers, which was also indicated in grain crack analysis data where distance of failure was higher than conventional leathers.

From Figure 2 organoleptic properties such as grain smoothness, grain tightness, fullness and visual appearance of B45 and B60 tanned leathers were comparable to that of conventional BCS treated leathers. B60 treated leathers had smoother grain and better visual appearance, on the other hand B45 treated leathers showed better fullness, grain tightness and better visual appearance than BCS treated leathers.

Conclusion

Chrome tanning material containing anionic chromium complex with suitable ligands have been prepared and employed in pickle-less chrome tanning of goat skins at elevated pH conditions eliminating the use of common salt and strong mineral acids. These chromium complexes owing to higher stability exhibited resistance to precipitation when offered to the de-limed pelt. Also, this new tanning material did not find any problem in penetrating into the collagen matrix and was evenly distributed over the surface. Moreover, due to the masking of coordinating sites, more amount of chromium was fixed to the collagen.

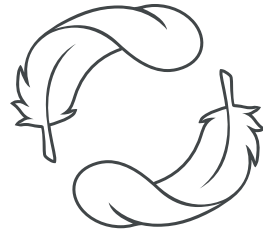
Experimental leathers thus produced have been found to have shrinkage temperature up to 105°C and exhibited 95% exhaustion. Pollution load assessment data shows that the B45 and B60 tanning materials have minimal impact on the environment than the conventional BCS tanning by eliminating use of acids and neutral salts in leather processing. This pickle less and self-basifying system opens new avenues for practising cleaner and safer chrome tanning process by minimising chromium metal in the effluent discharge.

Acknowledgement

Financial support from CSIR under Supra-institutional project STRAIT is acknowledged.

References

1. Karamali K., Ree T. V.; Tannins: Classification and Definition, *Nat. Prod. Rep.*, **18**, 641-649, 2001.
2. Schultz A.; Tawing hides and skins, US 291,784 A, Jan. 8, 1884.
3. Martin D.; Tanning-liquor, US 511,411, Dec. 26, 1893.
4. Willams D. A.; Method of treating chrome liquors, US 2,110,187, Aug. 23, 1933.
5. Sarkar K. T.; Theory and practice of leather manufacture, Revised Edition. 2012.
6. Rao J. R., Chandrasekaran B., Nair B. U., Ramasami T.; Eco-benign Management Options for Cleaner Chrome Tanning, *JSIR*, **61**(11), 912-926, 2002.
7. Ludvík J.; The scope for decreasing pollution load in leather processing. UNIDO, Regional Programme for Pollution Control in the Tanning Industry in South-East Asia, Aug. 9, 2000.
8. Cotton F. A., Wilkinson G., Murillo C. A., and Bochmann M.; *Advanced Inorganic Chemistry*, 6th Edition, 2000.
9. Ramasami T., Chandrababu N, K., Chandrasekaran B., Raghava Rao J., Kanthimathi M., Narasimhan V.; Approach towards low waste chrome tanning, Proceedings of 22nd Tanners get together, 167-199, 1987.
10. Rao J. R., Nair B. U., Ramasami, T.; Isolation and Characterization of Low Affinity Chromium(III) Complex in Chrome Tanning Solutions. *J.Soc.L Leather Technol.Chem.*, **81**, 234-238, 1997.
11. Chandrasekaran B., Rao J. R., Sreeram K. J., Nair B. U., Ramasami T., Chrome Tanning: State of art on the material composition and characterization, *JSIR*, **58**, 1-10, 1999.
12. Sreeram K. J., Ramasami T.; Sustaining tanning process through conservation, recovery and better utilization of chromium, *Resources, Conservation and Recycling*, **38**, 185-212, 2003.
13. Suresh V., Kanthimathi M., Thanikaivelan P., Raghava Rao J., Unni Nair B.; An improved product-process for cleaner chrome tanning in leather processing. *Journal of Cleaner Production*, **9**(6), 483-491, 2001.
14. Hervey L. R. B.; Process of preparing tanning material and by products derived from therefrom, US 2,178,874, May 6, 1937.
15. ASTM D6019-10, Test method for determination of chromic oxide in basic chromium tanning liquors (Ammonium Persulfate Oxidation), ASTM International, West Conshohocken, PA, 2010.
16. ASTM D1252-06, Standard test methods for chemical oxygen demand (dichromate oxygen demand) of water. ASTM International, West Conshohocken, PA, 2012.
17. APHA 2540B, Standard Methods for the Examination of Water and Wastewater, 17th edition, 1989.
18. IUP 2, Sampling, *JSLTC* **84**, 303, 2000.
19. IUP 6, Measurement of tensile strength and percentage elongation, *JSLTC* **84**, 317, 2000.
20. UNIDO, Acceptable quality standards in the leather and footwear industry, **34**, 1994.
21. ASTM D3897-9, Standard Practice for Calculation of Basicity of Chrome Tanning Liquors, ASTM International, West Conshohocken, PA, 2012.
22. Lunk H-J.; Discovery, properties and applications of chromium and its compounds. *ChemTexts* **1**, 6, 2015.



C O L D M i l l i n g



Smooth Leather
Milling

Lifelines

Jun Liu see *JALCA*, 2015, 110(1).

Da-hai He received his master's degree in organic chemistry from Southwest University for Nationalities (now Southwest Minzu University) in 2010, and his PhD in pharmaceutical chemistry from University of Chinese Academy of Science in 2013, during 2016-2017, he held a postdoctoral position at Ohio State University.

Hua-lin Chen see *JALCA*, 2017, 112(5).

Ke-yi Ding, see *JALCA*, 2015, 110(1).

Jie Liu received his PhD degree in 2007 from Institute of Mechanics, Chinese Academy of Sciences, Beijing, China. He currently is an associate professor at the School of Materials Science and Engineering at Zhengzhou University, Zhengzhou, China. From 2016 to 2017, he worked as a visiting scientist at ERRC, USDA in Cheng-Kung Liu's group. His current research interests focus on green composite materials based on natural polymers and their applications in packaging, biomedical and environmental fields

Yanchun Liu is a master's degree candidate at the School of Materials Science and Engineering at Zhengzhou University, Zhengzhou, China, majoring in materials science and engineering. She is engaged in the development of green packaging materials based on polysaccharides and proteins.

Eleanor Brown received a PhD in Chemistry from Drexel University in 1971. Upon graduation, she received a National Research Council postdoctoral fellowship to ERRC, ARS, USDA where she began the study of protein structure-function relationships in a variety of agriculturally important systems (dairy, poultry, and leather). Between 1985 and 1995 she was part of a small team that pioneered the molecular modeling of the non-crystalline proteins, collagen and the caseins. She has received numerous awards from the ALCA Prize paper in 1993, Alsop in 1996, and O'Flaherty in 2012. In 2013, she received the IULTCS Merit Award for Excellence in the Leather Industry. She retired from ERRC in 2018, and continues to work with colleagues there as a Collaborator

Zhengxin Ma is a master's degree candidate at the School of Materials Science and Engineering at Zhengzhou University, Zhengzhou, China, majoring in materials science and engineering. His research focus on the antimicrobial packaging materials based on polysaccharides.

Cheng-Kung Liu received his PhD. degree in Fiber and Polymer Science from North Carolina State University and Master and Bachelor degrees in Textile Engineering from Feng Chia University, Taiwan. He joined ARS, USDA in 1996 and has served as Research Materials Engineer, Lead scientist, and Research Leader at ERRC, Wyndmoor, PA. Dr. Liu's research efforts have been focusing on polymeric fibrous products, green composites, and nondestructive evaluation techniques. He has 110 refereed technical publications, 33 U.S. patents and 58 foreign patents.

J.M. Morera graduated in Chemistry at the University of Barcelona (Spain) in 1983. He got his PhD degree in Chemistry at the same University in 1994. He received the Master in Tanning Technical Management from the Universitat Politècnica de Catalunya (Spain) in 1999. From 1985 to 2018 he worked as an associate professor at the Universitat Politècnica de Catalunya (Spain). From 2018 to 2020 he worked as an associate professor at the Universitat de Lleida (Spain). Since 2020 he has been working as a full professor at the Universitat de Lleida (Spain). He is mainly involved in the development of cleaner and innovative leather processing methods.

E. Bartolí graduated in Chemistry at the University of Barcelona (Spain) in 1985. He got his PhD degree in Chemistry at the same University in 2000. He received the Master in Tanning Technical Management from the Universitat Politècnica de Catalunya (Spain) in 1999. From 1985 to 2018 he worked as an associate professor at the Universitat Politècnica de Catalunya (Spain). Since 2020 he has been working as a full professor at the Universitat de Lleida (Spain). She is mainly involved in the development of cleaner and innovative leather processing methods.

P. Rojas has been an Advanced App Engineering Analyst at Accenture since 2018. She graduated in Chemical Engineering at Polytechnic University of Catalonia (UPC) (Spain) in 2017. She had been working in 2016-2017 in quality analysis at ABC Leather S.L

L.F. Cabeza graduated in chemical engineering and industrial engineering at the University Ramon Llull (Barcelona, Spain) in 1993. She received an MBA degree in 1995 and her PhD in 1996 at the same university. From 1996 to 1998 she was a post-doctoral researcher at ERRC-ARS-USDA (Philadelphia, USA). In 1999 she joined the Universitat de Lleida (Spain), where she created and is leading the GREiA research group. Her research interests are on energy efficiency, circular economy, and social acceptance of technologies.

Obituary

David Rabinovich, age 83, passed away on July 1, 2021 in Las Cruces, New Mexico.



David was born January 18, 1938 in the Andean town of Medellín, Colombia, and received his primary and most of his secondary education at the Universidad Pontificia Bolivariana schools in Medellín. He attended the University of California at Berkeley where he received a BS in Chemistry (1962) and San José State College where he obtained a Master's in Chemistry in 1965. He worked since 1966 as a tanner in a family business, Andina de Curtidos, in the village of Copacabana just north of Medellín. He was involved in the founding of ACOLCUR, the Colombian Leather Chemists Association and was on the board of the CIDI's leather research institute at the Bolivariana; directing a Master's degree thesis on the use of chrome shavings as an ion-exchange resin to recover goldcyanide tailings and radioactive metals. He was in charge of research and development for the Titán Tannery in Cali, Colombia, from 1993 through 1995. In early 1996 he started working for J.H. Lowenstein & Sons, Brooklyn, NY, travelling mainly to India and Mexico, through 2006. Since 2007 he was a leather consultant, travelling primarily to Latin America for Grupo ABC Leder Andino SA, implementing low pollution processing, with zero sulphide/chrome in the effluents from tannery wet-end processes. In 1982 he presented a paper at the Latin-American Leather Chemists Congress, Bogotá, on the Colombian Cattle Slaughter Cycle. In November of 1982 he published a study

of weight/area yield for lime-split upper leather in Das Leder. In November 1995, at the XIII Latin-American Leather Chemists Congress at Cartagena, he presented a paper on Environmental Thermodynamics Implications for the Leather Industry. In 1999, during the IULTCS congress at Chennai, he presented a paper on low float, low effluent retannages. In 1999 he awarded by the Mexican Leather Chemists Association the San Jordi prize for academic excellence for a paper titled: "Seeking Soft Leather with Good Break", which lead to a publication in World Leather Magazine in 2002. He was appointed coeditor of a CLRI project for a Treatise on Leather Technology and assigned a chapter on the Material Science of Leather Making. His work on collagen reactivity, presented at the 105th ALCA Annual Convention, was part of the CLRI treatise assignment. He was a translator for JALCA Abstracts into Spanish and a member of ALCA since 1966. He became a life member of the ALCA in 2007. He served on the 2008 ALCA O'Flaherty Selection Committee and on the 2009 ALCA Alsop Selection Committee. He attended and presented at many of the ALCA Annual Conventions and was well known for his provocative and probing questions. In 2013 he was the Dr. Robert M. Lollar Prize Paper Award recipient and attended the XXXII IULTCS Congress May 29-31, 2013 in Istanbul, Turkey to give his paper titled "Everything You Wanted to Know about Collagen Models - But Were Too Afraid to Ask!" He was truly passionate about the leather industry as well as the ALCA; however, we have found out that he also had a passion, when he had time, for flying his Piper Cub and later his Cessna 180 private airplanes.

David married Marcia Lynn Slowinski, on February 22, 1963 in Reno, NV. She preceded him in death on June 29, 2010. He is survived by his two sons, Alexander and spouse Adriana of Glendale, CA and Victor and spouse Nicole of El Granada, CA.

INDEX TO ADVERTISERS

ALCA Annual Meeting	<i>Inside Back Cover</i>
Buckman Laboratories.	<i>Inside Front Cover</i>
Chemtan.	<i>Back Cover</i>
Chemtan.	338
Erretre	374



**116th ALCA
ANNUAL CONVENTION
Change of Date:
June 21–24, 2022
Eaglewood Resort & Spa
Itasca, IL**

**Featuring the 61st John Arthur Wilson Memorial Lecture
By Randy Johnson, President and CEO
of GST AutoLeather
Title: Road Ahead**

Tentative Schedule

Tuesday, June 21

Golf Tournament, Opening Reception and Dinner

Wednesday, June 22

***John Arthur Wilson Memorial Lecture
All Day Technical Sessions, Fun Run
Reception and Dinner, Activities - Bowling, Pool,
Darts and an Open Bar***

Thursday, June 23

***All Day Technical Sessions, Annual Business Meeting
Activities Awards Luncheon
Social Hour, ALCA Awards Banquet***

***Visit us at www.leatherchemists.org for full details
under Annual Convention as they become available***



***When leather feels this good,
the boots come off last!***



Leather chemistry for today.

Tel: (603) 772-3741 • Fax: (603) 772-0796
www.CHEMTAN.com

ISO 9001 Certified